VŠB - Technical University of Ostrava
Faculty of Electrical Engineering and Computer Science
Department of Applied Mathematics

Modelling of optical response from periodic systems

master thesis

2010

Lukáš Halagačka

I declare I elaborated this thesis by myself. All literary sources and publications I have used had been cited.

Ostrava, May 7, 2010 .....

I want to express my deep gratitude to my supervisor Dr. Kamil Postava from Department of Physic at the Technical University of Ostrava (TUO) who introduced me to the magic world of optics.

Abstract

This master thesis is focused to modeling of the optical response from periodical optial structures. The first part is devoted the Berreman and Yeh approach for solving the Maxwell equations in planar layers medium. Theoretical results are demonstrated on the system with sufrace plasmon resonance in the gold layer. The main part of the work is devoted to the modeling of one dimensional periodical structures with the RCWA (Rigorous Coupled Wave Analysis) method. Photonics crystals with non-reciprocity effect are modeled using using S-matrix algorithm. The effect of truncation Fourier series and Fourier factorization is demonstrated. Generalization of spectroscopic ellipsometry method for characterization of uniaxial anisotropic material is presented.

Keywords: planar layers, periodical structures, optical grating, RCWA, plasmon resonance, photonics crystal, ellipsometry

Abstrakt

Tato diplomová práce je zaměřena na modelování optické odezvy od periodických struktur. V první části jsou řešeny Maxwellovy rovnice pro struktury planárních vrstev pomoci Berremanova a Yehova přístupu. Výsledne vztahy jsou demonstrovovány na příkladu planární zlaté vrstvy s excitovanou plazmonovou resonancí. Hlavní část práce je věnována modelování periodických lamelárních (1D) mřížek pomoci metody vázaných vln, RCWA (Rigorous Coupled Wave Analysis). Pomoci S-maticového algoritmu je modelován fotonický krystal s nereciproými optickými vlastnostmi. Je diskutována přesnost výpočtu při použití konečného počtu členů Fourierovy aproximace nespojité funkce permitivity a metoda Fourierovy faktorizace pro zlepšení konvergence. Pro zpětnou charakterizaci materiálu je uvedeno zobecnění elipsometrických měření pro připad jednoosé anisotropie.

Klíčová slova: planární vrstvy, periodické struktůry, optická mřížka, RCWA, plasmonová rezonance, fotonický krystal, elipsometrie

Contents

List of Figures

1 Introduction

Thin films and periodic nanostructures found new applications in telecommunications and data storage technologies. In the line with the technical progresses in preparation process of the novel nanostructures it is necessary to evolve calculation methods for the modeling of optical response and field distribution.Example of application of the thin films technology are the metallic layers on the window-glass obstructing outside or inside heat radiation. Materials with the unusual effective optical properties can be designed as a periodical structures uses the plasmonic or the magnetoplasmonic resonance effect. Example of these advanced structures is the plasmonics structure with strong non-reciprocity effect. This structure has different propagation constant in one direction of propagation than in the opposite. In the telecommunications the optical insulator is used as a one-way optical filter protecting the device against backward reflected light. Because the actual conception of stand-alone (Figure. 1) optical insulator is bulky device which can not be integrated, it is necessary to design material structure with hight transmission in forward direction and strong attenuation in backward direction. This is a need for design and modeling of the structure, understanding of new physical phenomena, and efficient characterization of device prototype.

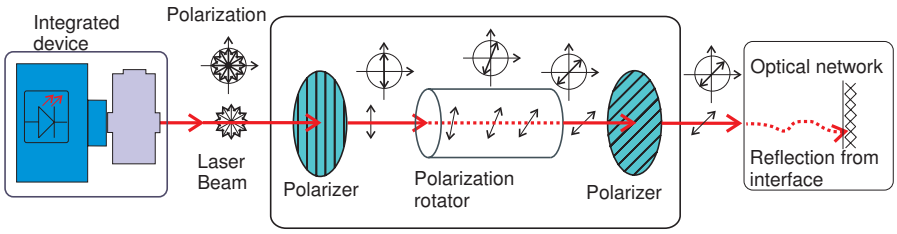

Figure 1: Conception of the stand alone optical insulator in telecommunication.

Objective of this work is modeling optical response from the system of planar layers and from the optical one-dimensional gratings. If we talking about light and its interaction with medium, it is obvious that there are two basic approaches for solving the Maxwell equations. First was introduced by D. W. Berreman in 1972, [1], and the second by P. Yeh in 1979, [2]. Both approaches are based on Maxwell equations and have the same results, but the keynote is different which gives us possibility for the derivation of analytical formulas in some special cases. Modeling of optical response from the one-dimensional gratings is little more complicated because of discontinuity of permitivity. The way for solving this discontinuous structures is the rigorous coupled wave analysis (RCWA), [3, 4]. For effective numerical calculation L. Li introduced advanced algorithms based on recursive S-matric algorithm [5, 6]. Beside numerical modeling of structure an experimental feedback between models and fabricated materials is needed. Spectroscpic ellipsometry [7, 8] is one of efficient optical methods for characterization thin films and nanostructures and is based on detection of changes in reflected polarized light. The measured signals are directly connected to the Jones reflection matrix of the sample. This method is usualy applied to the both isotropic materials [9]. Characterization of anisotropic materials using phase modulated method is elaborated in this work.

This master thesis consist of tree main chapters. *Chapter* 2. summarizes transformation of

Maxwell equations into form used in the Berreman and Yeh approach. Using the continuity of the electric and magnetic field tangential components at the planar interface the M-matrix algorithm is introduced. Using the mathematical approach the the planar structure with excited surface plasmon resonance is modeled. In *Chapter* 3. the theoretical knowledge of solving Maxwell equations is applied to the one-dimensional (1D) lammelar gratings. For the expression of the field inside periodical structure the truncated Fourier series of the permitivity tensor is introduced using the RCWA method. Implementation of the code for 1D grating based on MATLAB software is the most important result of this master thesis. Numerical stability and convergence is improved using the scattering matrix algorithm for the one-dimensional gratings and the Fourier Factorization method. The effect of truncation Fourier series is demonstrated on the example as well as the improvement of the convergence with the Fourier factorization method. The main result of this chapter is modeling optical periodical structures and presentation of photonics crystal with strong nonreciprocity effect. After the designing and modeling the new structures and their fabrication we have to characterize it using, for example, optical ellipsometry. *Chapter* 4. is devoted generalization of the spectroscopic ellipsometry to characterize anisotropic samples. The method is demonstrated on example of the uniaxial anisotropic crystal of the $\mathrm{SnO_2}$.

2 Theoretical background

2.1 Maxwell equations

Electromagnetic field and its interactions with surroundings is described by a set of the Maxwell equations defining the relations between the electric field $\mathbf{E}(\mathbf{r},t)$, the magnetic field $\mathbf{H}(\mathbf{r},t)$, the electric displacement $\mathbf{D}(\mathbf{r},t)$, the magnetic flux volume density $\mathbf{B}(\mathbf{r},t)$, the density volume of the free charges $\rho(\mathbf{r},t)$, the and current density $\mathbf{j}(\mathbf{r},t)$:

$$\nabla \times \mathbf{H}(\mathbf{r},t) = \mathbf{j}(\mathbf{r},t) + \frac{\partial \mathbf{D}(\mathbf{r},t)}{\partial t}, \tag{2.1a}$$

$$\nabla \times \mathbf{E}(\mathbf{r},t) = -\frac{\partial \mathbf{B}(\mathbf{r},t)}{\partial t}, \tag{2.1b}$$

$$\nabla \cdot \mathbf{D}(\mathbf{r},t) = \rho(\mathbf{r},t), \tag{2.1c}$$

$$\nabla \cdot \mathbf{B}(\mathbf{r},t) = 0, \tag{2.1d}$$

and additional constitution relations between the polarization $\mathbf{P}(\mathbf{t},t)$ and the magnetization $\mathbf{M}(\mathbf{r},t)$ volume density:

$$\mathbf{D}(\mathbf{r},t) = \epsilon_0 \mathbf{E}(\mathbf{r},t) + \mathbf{P}(\mathbf{r},t), \tag{2.2a}$$

$$\mathbf{B}(\mathbf{r},t) = \mu_0 \mathbf{H}(\mathbf{r},t) + \mu_0 \mathbf{M}(\mathbf{r},t), \tag{2.2b}$$

μ_0 is the free space permeability and ϵ_0 is the free space permitivity. At following calculations let's consider magnetization volume density for optical frequencies $\mathbf{M} = 0$ and linear material properties without free charges at the interfaces:

$$\boldsymbol{\rho}(\mathbf{r},t) = 0. \tag{2.3}$$

The charge volume density $\mathbf{j}$ can be expressed using conductivity tensor $\hat{\sigma}$ by relation:

$$\mathbf{j}(\mathbf{r},t) = \hat{\sigma}\mathbf{E}(\mathbf{r},t). \tag{2.4}$$

Using tensor of the electric susceptibility $\hat{\chi_e}$ defining relation between the polarization volume density and electric intensity:

$$\mathbf{P}(\mathbf{r},t) = \epsilon_0 \hat{\chi_e} \mathbf{E}(\mathbf{r},t), \tag{2.5}$$

we defined the permitivity tensor $\hat{\epsilon}$:

$$\hat{\epsilon} = \epsilon_0 \left(\hat{\mathbb{I}} + \hat{\chi_e}\right) = \epsilon_0 \hat{\epsilon_R}. \tag{2.6}$$

Those premises let's us write Maxwell equations (2.1a - 2.1d) in the new form:

$$\nabla \times \mathbf{H}(\mathbf{r},t) = \hat{\epsilon}\frac{\partial \mathbf{E}(\mathbf{r},t)}{\partial t} + \hat{\sigma}\mathbf{E}(\mathbf{r},t), \tag{2.7a}$$

$$\nabla \times \mathbf{E}(\mathbf{r},t) = -\mu_0 \frac{\partial \mathbf{H}(\mathbf{r},t)}{\partial t}, \tag{2.7b}$$

$$\nabla \cdot [\hat{\epsilon}\mathbf{E}(\mathbf{r},t)] = 0, \tag{2.7c}$$

$$\nabla \cdot \mathbf{H}(\mathbf{r},t) = 0. \tag{2.7d}$$

During following calculations let impeach only monochromatic plane waves and separation of time- and space-dependency. Than the electric and magnetic field vector can be expressed in form:

$$\mathbf{E}(\mathbf{r},t) = E_0\mathbf{e}\exp\left(\mathrm{i}\left(\mathbf{kr}-\omega t\right)\right) = \mathbf{E}(\mathbf{r})\exp\left(-\mathrm{i}\omega t\right), \tag{2.8a}$$

$$\mathbf{H}(\mathbf{r},t) = H_0\mathbf{h}\exp\left(\mathrm{i}\left(\mathbf{kr}-\omega t\right)\right) = \mathbf{H}(\mathbf{r})\exp\left(-\mathrm{i}\omega t\right), \tag{2.8b}$$

where $\omega = \frac{2\pi}{\lambda}$, λ is the wavelength, complex constants E_0, H_0 are time and space independent amplitudes and $\mathbf{e}, \mathbf{h}$ are polarization vectors time and space independent as well. Relations (2.8aa,b) used in (2.7) leads to time-dependency elimination:

$$\nabla \times \mathbf{H}(\mathbf{r}) = -\mathrm{i}\omega\hat{\epsilon}\mathbf{E}(\mathbf{r}) + \hat{\sigma}\mathbf{E}(\mathbf{r}), \tag{2.9a}$$

$$\nabla \times \mathbf{E}(\mathbf{r},t) = \mathrm{i}\omega\mu_0\mathbf{H}(\mathbf{r}). \tag{2.9b}$$

Final form of Maxwell's equations is obtained with complex permitivity tensor $\hat{\epsilon}'$ in equation (2.9a):

$$\hat{\epsilon}' = \hat{\epsilon} + \frac{\mathrm{i}}{\omega}\hat{\sigma}, \tag{2.10}$$

This tensor describes optical properties of any anisotropic material. In case of absorbing material the imaginary part of complex permitivity tensor is nonzero, $\Im\hat{\epsilon}' \neq 0$. Therefore final expression of Maxwell equations in the form:

$$\nabla \times \mathbf{H}(\mathbf{r}) = -\mathrm{i}\omega\hat{\epsilon}'\mathbf{E}(\mathbf{r}), \tag{2.11a}$$

$$\nabla \times \mathbf{E}(\mathbf{r},t) = \mathrm{i}\omega\mu_0\mathbf{H}(\mathbf{r}), \tag{2.11b}$$

$$\nabla \cdot [\hat{\epsilon}\mathbf{E}(\mathbf{r},t)] = 0, \tag{2.11c}$$

$$\nabla \cdot \mathbf{H}(\mathbf{r},t) = 0, \tag{2.11d}$$

describing any absorbing or non-absorbing linear homogeneous non-dispersive anisotropic material.

2.2 Polarized light

Light is an electromagnetic wave defined by vector of electric and magnetic intensity connected together with Maxwell's equations (2.11). For monochromatic plane wave these vectors can be expressed in form:

$$\begin{aligned}\mathbf{E}(\mathbf{r},t) &= E_0\mathbf{e}\exp\left(\left[\mathrm{i}\left(\mathbf{k}\cdot\mathbf{r}-\omega t\right)\right]\right),\\ \mathbf{H}(\mathbf{r},t) &= H_0\mathbf{h}\exp\left(\left[\mathrm{i}\left(\mathbf{k}\cdot\mathbf{r}-\omega t\right)\right]\right).\end{aligned} \tag{2.12}$$

With respect to complementarity of electric and magnetic field intensity $\mathbf{E}, \mathbf{H}$ (see eq.(2.11a,2.11b)), following derivations will be done only for electric field $\mathbf{E}$. Real part of wave vector $\Re\{\mathbf{k}\}$ represents direction of propagation and imaginary $\Im\{\mathbf{k}\}$ effects increasing or decaying of amplitude. Vector $\mathbf{e}$ is the polarization vector. In general case it is the elliptical polarization (ending point of vector copying out the ellipse). In right-handed cartesian system of coordinates with z-axis parallel to $\mathbf{k}$ vector the plane wave polarization ellipse is perpendicular to direction of propagation (z-axis). In common configuration in calculations and experiments the system of coordinates is chosen with respect to perpendicularity x-axis to plane of incidence-plane of incidence is $y-z$ plane (Figure 3.). In that

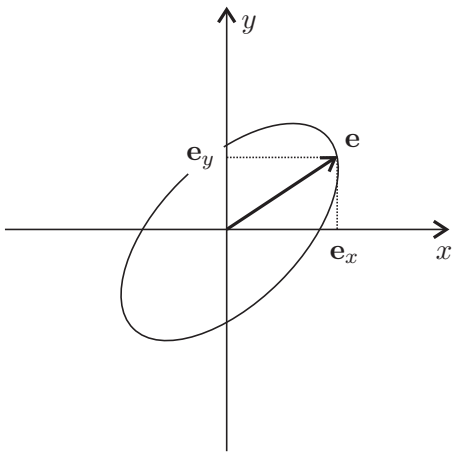

Figure 2: Real part of elliptically polarized vector $\mathbf{e}$, propagation in z-axis direction.

geometry there are two significant polarizations. S-polarization (**TE**, Transversal Electric, $\mathbf{e}$ perpendicular to plane of incidence) and p-polarization (**TM**, Transversal Magnetic, $\mathbf{e}$ parallel with plane of incidence). Because of orthogonality of the s- and p-polarizations, any

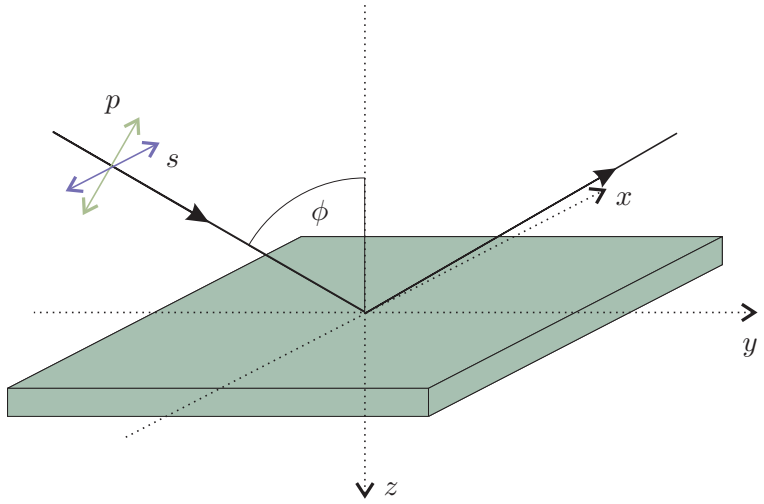

Figure 3: s- and p-polarization in system of coordinates.

linear polarized wave could be determined by linear combination of them. According to Jones formalism [10]:

$$\mathbf{e} = \begin{bmatrix} \mathbf{e}_x \\ \mathbf{e}_y \end{bmatrix} = \begin{bmatrix} e_x \mathrm{e}^{i\varphi_x} \\ e_y \mathrm{e}^{i\varphi_y} \end{bmatrix} \tag{2.13}$$

the s- and p-polarization is represented by the vector:

$$\mathbf{e}_s = \begin{bmatrix} 1 \\ 0 \end{bmatrix}, \quad \mathbf{e}_p = \begin{bmatrix} 0 \\ 1 \end{bmatrix}. \tag{2.14}$$

2.3 Material parameters

Optical response of material is effected by material parameters, which are permitivity ϵ and permeability μ. For optical frequencies the permeability is equal permeability of the free space, $\mu = \mu_0$. Tensor of permeability in (2.11a) is in general in form:

$$\hat{\epsilon}_R^{'} = \begin{bmatrix} \epsilon_{xx} & \epsilon_{xy} & \epsilon_{xz} \\ \epsilon_{yx} & \epsilon_{yy} & \epsilon_{yz} \\ \epsilon_{zx} & \epsilon_{zy} & \epsilon_{zz} \end{bmatrix}. \tag{2.15}$$

Form of general anisotropic tensor can be reduced into simplest form:

- **Isotropic material**
  Isotropic material has rotation symmetry around all exes:

$$\hat{\epsilon}_R^{'} = \begin{bmatrix} \epsilon_{xx} & 0 & 0 \\ 0 & \epsilon_{xx} & 0 \\ 0 & 0 & \epsilon_{xx} \end{bmatrix}. \tag{2.16}$$

- **Uniaxial anisotropy**
  Uniaxial anisotropic material has rotation symmetry around one symmetry axis, in the following case the y-axes:

$$\hat{\epsilon}_R^{'} = \begin{bmatrix} \epsilon_{xx} & 0 & 0 \\ 0 & \epsilon_{yy} & 0 \\ 0 & 0 & \epsilon_{xx} \end{bmatrix}. \tag{2.17}$$

- **Biaxial anisotropy**
  Tensor of biaxial anisotropic material has all diagonal elements different:

$$\hat{\epsilon_R^{'}} = \begin{bmatrix} \epsilon_{xx} & 0 & 0 \\ 0 & \epsilon_{yy} & 0 \\ 0 & 0 & \epsilon_{zz} \end{bmatrix}. \tag{2.18}$$

Effect when the permitivity tensor depends on outer magnetic field is called Magneto-optic effect. If the dependency is linear - characterized with *Voight* parameter q, there are three basic anisotropic configurations:

- **Polar configuration**

$$\epsilon_{xx} \begin{bmatrix} 1 & -\mathrm{i}q & 0 \\ \mathrm{i}q & 1 & 0 \\ 0 & 0 & 1 \end{bmatrix}, \tag{2.19}$$

- **Longitudinal configuration**

$$\epsilon_{xx}\begin{bmatrix} 1 & 0 & \mathrm{i}q \\ 0 & 1 & 0 \\ -\mathrm{i}q & 0 & 1 \end{bmatrix}, \tag{2.20}$$

- **Transversal configuration**

$$\epsilon_{xx}\begin{bmatrix} 1 & 0 & 0 \\ 0 & 1 & -\mathrm{i}q \\ 0 & \mathrm{i}q & 1 \end{bmatrix}. \tag{2.21}$$

If the space orientation of tensor does not corresponds with specified system of coordinates it can be transformed by rotation matrix R:

$$\hat{\epsilon}_{\mathrm{rot}} = \mathrm{R}^{-1}\hat{\epsilon}\mathrm{R} \tag{2.22}$$

Each rotation transformation can be described with combination of rotation around all axes apart: Rotation matrix around x axis with angle φ, y with α and z with β has form:

$$\mathrm{R}(\varphi,\alpha,\beta) = \begin{bmatrix} \cos\varphi & -\sin\varphi & 0 \\ \sin\varphi & \cos\varphi & 0 \\ 0 & 0 & 1 \end{bmatrix}\begin{bmatrix} 1 & 0 & 0 \\ 0 & \cos\alpha & \sin\alpha \\ 0 & -\sin\alpha & \cos\alpha \end{bmatrix}\begin{bmatrix} \cos\beta & 0 & -\sin\beta \\ 0 & 1 & 0 \\ \sin\beta & 0 & \cos\beta \end{bmatrix} \tag{2.23}$$

2.4 Solving Maxwell equations in planar structure

Berreman (and Yeh (2.4.2)) approach to finding solutions of Maxwell equations (2.11) is based on continuity of tangential component of the electric field $\mathbf{E}$ and magnetic field $\mathbf{H}$ on the plane interface between two media. From continuity fact comes out the idea of solving sets of Maxwell equations only for their tangential components and recalculate normal components from them.

2.4.1 Berreman approach for solving Maxwell equations

Berreman calculation [1] starts from (2.11a,2.11b) and expand them into system of linear differential equations with constant coefficients. Is necessary to do a few transformations to get final form of system of equation. First step is applying normalization:

$$\mathbf{E}'(\mathbf{r}) = \sqrt[4]{\mu_0^{-1}\epsilon_0}\mathbf{E}(\mathbf{r}), \tag{2.24a}$$

$$\mathbf{H}'(\mathbf{r}) = \sqrt[4]{\epsilon_0^{-1}\mu_0}\mathbf{H}(\mathbf{r}), \tag{2.24b}$$

into (2.11a,2.11b):

$$\nabla\times\mathbf{H}'(\mathbf{r}) = -\mathrm{i}k_0\hat{\epsilon}\mathbf{E}'(\mathbf{r}), \tag{2.25a}$$

$$\nabla\times\mathbf{E}'(\mathbf{r},t) = \mathrm{i}k_0\mathbf{H}'(\mathbf{r}), \tag{2.25b}$$

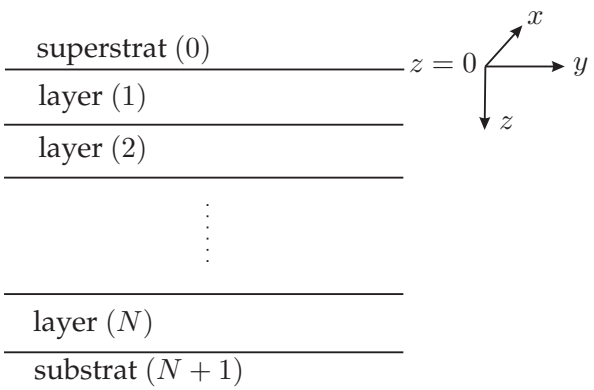

Figure 4: System of coordinates for planar structure

where $k_0 = \frac{\omega}{c}$ is the amplitude of wave vector in the free space. With general permitivity tensor (2.15) equations could be written with matrix notation in form:

$$\begin{bmatrix} 0 & 0 & 0 & 0 & -\frac{\partial}{\partial z} & \frac{\partial}{\partial y} \\ 0 & 0 & 0 & \frac{\partial}{\partial z} & 0 & -\frac{\partial}{\partial x} \\ 0 & 0 & 0 & -\frac{\partial}{\partial y} & \frac{\partial}{\partial x} & 0 \\ 0 & -\frac{\partial}{\partial z} & \frac{\partial}{\partial y} & 0 & 0 & 0 \\ \frac{\partial}{\partial z} & 0 & -\frac{\partial}{\partial x} & 0 & 0 & 0 \\ -\frac{\partial}{\partial y} & \frac{\partial}{\partial x} & 0 & 0 & 0 & 0 \end{bmatrix} \begin{bmatrix} \mathbf{E}'_x(\mathbf{r}) \\ \mathbf{E}'_y(\mathbf{r}) \\ \mathbf{E}'_z(\mathbf{r}) \\ \mathbf{H}'_x(\mathbf{r}) \\ \mathbf{H}'_y(\mathbf{r}) \\ \mathbf{H}'_z(\mathbf{r}) \end{bmatrix} =$$

$$= \mathrm{i}k_0 \begin{bmatrix} -\epsilon_{xx} & -\epsilon_{xy} & -\epsilon_{xz} & 0 & 0 & 0 \\ -\epsilon_{yx} & -\epsilon_{yy} & -\epsilon_{yz} & 0 & 0 & 0 \\ -\epsilon_{zx} & -\epsilon_{zy} & -\epsilon_{zz} & 0 & 0 & 0 \\ 0 & 0 & 0 & 1 & 0 & 0 \\ 0 & 0 & 0 & 0 & 1 & 0 \\ 0 & 0 & 0 & 0 & 0 & 1 \end{bmatrix} \begin{bmatrix} \mathbf{E}'_x(\mathbf{r}) \\ \mathbf{E}'_y(\mathbf{r}) \\ \mathbf{E}'_z(\mathbf{r}) \\ \mathbf{H}'_x(\mathbf{r}) \\ \mathbf{H}'_y(\mathbf{r}) \\ \mathbf{H}'_z(\mathbf{r}) \end{bmatrix}. \tag{2.26}$$

With respect to the structure and the system of coordinates (see Fig.4), solving plane waves would be constant at $x - y$ plane:

$$\mathbf{E}'(\mathbf{r}) = E'_0 \mathbf{e}' \exp\left(\mathrm{i}k_0\left(\nu_x x + \nu_y y\right)\right), \tag{2.27a}$$

$$\mathbf{H}'(\mathbf{r}) = H'_0 \mathbf{h}' \exp\left(\mathrm{i}k_0\left(\nu_x x + \nu_y y\right)\right), \tag{2.27b}$$

which lead to constant derivation in direction of tangential components and electromagnetic field in structure is a function of z-coorinate:

$$\begin{bmatrix} 0 & 0 & 0 & 0 & -\frac{\partial}{\partial z} & \mathrm{i}k_0\nu_y \\ 0 & 0 & 0 & \frac{\partial}{\partial z} & 0 & -\mathrm{i}k_0\nu_x \\ 0 & 0 & 0 & -\mathrm{i}k_0\nu_y & \mathrm{i}k_0\nu_x & 0 \\ 0 & -\frac{\partial}{\partial z} & \mathrm{i}k_0\nu_y & 0 & 0 & 0 \\ \frac{\partial}{\partial z} & 0 & -\mathrm{i}k_0\nu_x & 0 & 0 & 0 \\ -\mathrm{i}k_0\nu_y & \mathrm{i}k_0\nu_x & 0 & 0 & 0 & 0 \end{bmatrix} \begin{bmatrix} \mathbf{e}_x^{'} \\ \mathbf{e}_y^{'} \\ \mathbf{e}_z^{'} \\ \mathbf{h}_x^{'} \\ \mathbf{h}_y^{'} \\ \mathbf{h}_z^{'} \end{bmatrix} =$$

$$= \mathrm{i}k_0 \begin{bmatrix} -\epsilon_{xx} & -\epsilon_{xy} & -\epsilon_{xz} & 0 & 0 & 0 \\ -\epsilon_{yx} & -\epsilon_{yy} & -\epsilon_{yz} & 0 & 0 & 0 \\ -\epsilon_{zx} & -\epsilon_{zy} & -\epsilon_{zz} & 0 & 0 & 0 \\ 0 & 0 & 0 & 1 & 0 & 0 \\ 0 & 0 & 0 & 0 & 1 & 0 \\ 0 & 0 & 0 & 0 & 0 & 1 \end{bmatrix} \begin{bmatrix} \mathbf{e}_x^{'} \\ \mathbf{e}_y^{'} \\ \mathbf{e}_z^{'} \\ \mathbf{h}_x^{'} \\ \mathbf{h}_y^{'} \\ \mathbf{h}_z^{'} \end{bmatrix}, \tag{2.28}$$

where ν_x, ν_y are the components of normalized wave vector $\mathbf{k}$:

$$\mathbf{k} = k_0 \left(\mathbf{i}\nu_x + \mathbf{j}\nu_y + \mathbf{k}\nu_z \right). \tag{2.29}$$

Dependency of z-components on $x-$, y-components coming out from (2.28) could be written:

$$\begin{bmatrix} 0 & 0 & 0 & -\mathrm{i}k_0\nu_y & \mathrm{i}k_0\nu_x & 0 \\ -\mathrm{i}k_0\nu_y & \mathrm{i}k_0\nu_x & 0 & 0 & 0 & 0 \end{bmatrix} \begin{bmatrix} \mathbf{e}_x^{'} \\ \mathbf{e}_y^{'} \\ \mathbf{e}_z^{'} \\ \mathbf{h}_x^{'} \\ \mathbf{h}_y^{'} \\ \mathbf{h}_z^{'} \end{bmatrix} = \mathrm{i}k_0 \begin{bmatrix} -\epsilon_{zx} & -\epsilon_{zy} & -\epsilon_{zz} & 0 & 0 & 0 \\ 0 & 0 & 0 & 0 & 0 & 1 \end{bmatrix} \begin{bmatrix} \mathbf{e}_x^{'} \\ \mathbf{e}_y^{'} \\ \mathbf{e}_z^{'} \\ \mathbf{h}_x^{'} \\ \mathbf{h}_y^{'} \\ \mathbf{h}_z^{'} \end{bmatrix}. \tag{2.30}$$

Before following deductions let's introduce vector of tangential components $\mathbf{F}(z)$ depending on z-direction:

$$\mathbf{F}(z) = \left[\mathbf{e}_x^{'}(z), \mathbf{h}_y^{'}(z), \mathbf{e}_y^{'}(z), \mathbf{h}_x^{'}(z) \right]^T, \tag{2.31}$$

Using **F**-vector it is possible to obtain explicit formulas for normal components $\mathbf{e}_z^{'}, \mathbf{h}_z^{'}$:

$$\begin{bmatrix} -\epsilon_{zz}^{-1}\epsilon_{zx} & -\epsilon_{zz}^{-1}\nu_x & -\epsilon_{zz}^{-1}\epsilon_{zy} & \epsilon_{zz}^{-1}\nu_y \\ -\nu_y & 0 & \nu_x & 0 \end{bmatrix} \underbrace{\begin{bmatrix} \mathbf{e}_x^{'} \\ \mathbf{h}_y^{'} \\ \mathbf{e}_y^{'} \\ \mathbf{h}_x^{'} \end{bmatrix}}_{\mathbf{F}(z)} = \begin{bmatrix} \mathbf{e}_z^{'} \\ \mathbf{h}_z^{'} \end{bmatrix}. \tag{2.32}$$

Normal components relations used in (2.28) leads to dependency reduction on z-direction. System of four differential equations (4×4) is obtained ant it is solvable with different techniques. By proper reorganization is possible to transform this problem into eigenvalue problem and it should be easy numerically solved.

Tangential component can be written in the same way as normal (2.32):

$$\begin{bmatrix} 0 & 0 & 0 & -\frac{\partial}{\partial z} \\ 0 & 0 & \frac{\partial}{\partial z} & 0 \\ 0 & -\frac{\partial}{\partial z} & 0 & 0 \\ \frac{\partial}{\partial z} & 0 & 0 & 0 \end{bmatrix} \begin{bmatrix} \mathbf{e}_x^{'} \\ \mathbf{e}_y^{'} \\ \mathbf{h}_x^{'} \\ \mathbf{h}_y^{'} \end{bmatrix} + \mathrm{i}k_0 \begin{bmatrix} \nu_y \mathbf{e}_z^{'} \\ -\nu_x \mathbf{e}_z^{'} \\ \nu_y \mathbf{h}_z^{'} \\ -\nu_x \mathbf{h}_z^{'} \end{bmatrix} =$$

$$= \mathrm{i}k_0 \begin{bmatrix} -\epsilon_{xx} & -\epsilon_{xy} & 0 & 0 \\ -\epsilon_{yx} & -\epsilon_{yy} & 0 & 0 \\ 0 & 0 & 1 & 0 \\ 0 & 0 & 0 & 1 \end{bmatrix} \begin{bmatrix} \mathbf{e}_x^{'} \\ \mathbf{e}_y^{'} \\ \mathbf{h}_x^{'} \\ \mathbf{h}_y^{'} \end{bmatrix} + \begin{bmatrix} -\epsilon_{xz}\mathbf{e}_z^{'} \\ \epsilon_{yz}\mathbf{e}_z^{'} \end{bmatrix}. \tag{2.33}$$

The system is reorganized with respect to the vector $\mathbf{F}(z)$ (2.31) substitutions $\mathbf{e}_z^{'}$, $\mathbf{e}_z^{'}$ according to (2.32) are used:

$$\left[\begin{bmatrix} 0 & -\frac{\partial}{\partial z} & 0 & 0 \\ 0 & 0 & 0 & \frac{\partial}{\partial z} \\ 0 & 0 & -\frac{\partial}{\partial z} & 0 \\ \frac{\partial}{\partial z} & 0 & 0 & 0 \end{bmatrix} + \mathrm{i}k_0 \begin{bmatrix} -\nu_y^2 & 0 & \nu_y\nu_x & 0 \\ \nu_y\nu_x & 0 & -\nu_x^2 & 0 \\ -\nu_y\epsilon_{zz}^{-1}\epsilon_{zx} & -\nu_y\epsilon_{zz}^{-1}\nu_x & -\nu_y\epsilon_{zz}^{-1}\epsilon_{zy} & \nu_y\epsilon_{zz}^{-1}\nu_y \\ \nu_x\epsilon_{zz}^{-1}\epsilon_{zx} & \nu_x\epsilon_{zz}^{-1}\nu_x & \nu_x\epsilon_{zz}^{-1}\epsilon_{zy} & \nu_x\epsilon_{zz}^{-1}\nu_y \end{bmatrix}\right] \mathbf{F}(z) =$$

$$= \left[\begin{bmatrix} -\epsilon_{xx} & 0 & -\epsilon_{xy} & 0 \\ -\epsilon_{yx} & 0 & -\epsilon_{yy} & 0 \\ 0 & 0 & 0 & 1 \\ 0 & 1 & 0 & 0 \end{bmatrix} \begin{bmatrix} \epsilon_{xz}\epsilon_{zz}^{-1}\epsilon_{zx} & \epsilon_{xz}\epsilon_{zz}^{-1}\nu_x & \epsilon_{xz}\epsilon_{zz}^{-1}\epsilon_{zy} & -\epsilon_{xz}\epsilon_{zz}^{-1}\nu_y \\ \epsilon_{yx}\epsilon_{zz}^{-1}\epsilon_{zx} & \epsilon_{yz}\epsilon_{zz}^{-1}\nu_x & \epsilon_{yz}\epsilon_{zz}^{-1}\epsilon_{zx} & -\epsilon_{yz}\epsilon_{zz}^{-1}\nu_y \\ 0 & 0 & 0 & 0 \\ 0 & 0 & 0 & 0 \end{bmatrix}\right] \mathrm{i}k_0\mathbf{F}(z). \tag{2.34}$$

Final form of eigenvalue problem:

$$\frac{\partial}{\partial z}\mathbf{F}(z) = \mathrm{i}k_0 \mathrm{C}\mathbf{F}(z), \tag{2.35}$$

where matrix C comes out (2.34):

$$\mathrm{C} = \begin{bmatrix} -\nu_x\epsilon_{zz}^{-1}\epsilon_{zx} & 1-\nu_x\epsilon_{zz}^{-1}\nu_x & -\nu_x\epsilon_{zz}^{-1}\epsilon_{zy} & \nu_x\epsilon_{zz}^{-1}\nu_y \\ -\nu_y^2+\epsilon_{xx}-\epsilon_{xz}\epsilon_{zz}^{-1}\epsilon_{zx} & -\epsilon_{xz}\epsilon_{zz}^{-1}\nu_x & \nu_y\nu_x+\epsilon_{xy}-\epsilon_{xz}\epsilon_{zz}^{-1}\epsilon_{zy} & \epsilon_{xz}\epsilon_{zz}^{-1}\nu_y \\ -\nu_y\epsilon_{zz}^{-1}\epsilon_{zx} & -\nu_y\epsilon_{zz}^{-1}\nu_x & -\nu_y\epsilon_{zz}^{-1}\epsilon_{zy} & \nu_y\epsilon_{zz}^{-1}\nu_y-1 \\ -\nu_x\nu_y-\epsilon_{yx}+\epsilon_{yz}\epsilon_{zz}^{-1}\epsilon_{zx} & \epsilon_{yz}\epsilon_{zz}^{-1}\nu_x & \nu_x^2+\epsilon_{yy}-\epsilon_{yz}\epsilon_{zz}^{-1}\epsilon_{zy} & -\epsilon_{yz}\epsilon_{zz}^{-1}\nu_y \end{bmatrix}. \tag{2.36}$$

Equation (2.35) is soluble as an eigenvalue problem of C matrix.
Eigenvalue decomposition:

$$\mathrm{CT} = \mathrm{VT}, \tag{2.37}$$

where T is column matrix of eigenvector and V is diagonal matrix of eigenvalues. Because of linear independence of eigenvectors, any vector which is in conformity with Maxwell equations (2.11) can be expressed as linear combination of eigenvectors and vector of amplitudes $\mathbf{g}(z)$:

$$\mathbf{F}(z) = \mathrm{T}\mathbf{g}(z). \tag{2.38}$$

Final system of differential equations for amplitudes vector is obtained by substituting (2.38) do (2.35):

$$\frac{\partial}{\partial z}\mathbf{g}(z) = \mathrm{i}k_0\mathrm{V}\mathbf{g}(z), \tag{2.39}$$

and the solution $g(z)$ can be written:

$$\mathbf{g}(z) = \exp(\mathrm{i}k_0 z_i \mathrm{V})\,\mathbf{A}, \tag{2.40}$$

where $\mathbf{A}$ is the vector of amplitudes on i-th interface, and $z_i = \in \langle 0, d_i \rangle$ is the z-coordinate at i-th layer.

Example 2.4.1
T and V matrices of isotropic homogeneous material
Let the plane of incidence wave is identical with $y-z$ plane (according to Figure. 3) and the medium is isotropic and homogeneous. Than component of normalized wave vector $\nu_x = 0$, permitivity tensor $\hat{\epsilon}$ is a diagonal matrix, $\hat{\epsilon} = diag(\epsilon, \epsilon, \epsilon)$ and C matrix describing this medium can be written in form:

$$\mathrm{C}_{iso} = \begin{bmatrix} 0 & 1 & 0 & 0 \\ \epsilon-\nu_y^2 & 0 & 0 & 0 \\ 0 & 0 & 0 & \nu_y\epsilon^{-1}\nu_y-1 \\ 0 & 0 & -\epsilon & 0 \end{bmatrix}. \tag{2.41}$$

The next step is calculation eigenvalues V_{iso} and eigenvectors T_{iso} of matrix C_{iso}. Analytical

formulas are necessary because of knowledge of ordering up and down vectors.

$$\mathrm{V}_{iso} = \begin{bmatrix} \sqrt{\epsilon - \nu_y^2} & 0 & 0 & 0 \\ 0 & -\sqrt{\epsilon - \nu_y^2} & 0 & 0 \\ 0 & 0 & \sqrt{\epsilon - \nu_y^2} & 0 \\ 0 & 0 & 0 & -\sqrt{\epsilon - \nu_y^2} \end{bmatrix}, \tag{2.42}$$

$$\mathrm{T}_{iso} = \begin{bmatrix} 1 & 1 & 0 & 0 \\ \sqrt{\epsilon - \nu_y^2} & -\sqrt{\epsilon - \nu_y^2} & 0 & 0 \\ 0 & 0 & (\sqrt{\epsilon})^{-1}\sqrt{\epsilon - \nu_y^2} & (\sqrt{\epsilon})^{-1}\sqrt{\epsilon - \nu_y^2} \\ 0 & 0 & -\sqrt{\epsilon} & \sqrt{\epsilon} \end{bmatrix}. \tag{2.43}$$

Considering to vector of the tangential components $\mathbf{F}$ (2.31) are column vectors at matrix $\mathrm{T_{iso}}$ organized by following way:

$$\mathrm{T}_{iso} = [S_{down}, S_{up}, P_{down}, P_{up}] \tag{2.44}$$

■

2.4.2 Yeh approach for solving Maxwell equations

Another way how to solve the electromagnetic wave propagating in anisotropic medium has been introduced by Yeh [2, 11]. Instead of solving system of linear differential first-order equations, the system is conversed into one second-order equation. With the aid of Yeh approach is easy to get analytical formulas for some special mediums. For example isotropic homogeneous media or media with special anisotropy caused by external magnetic field. Firstly the Helmholtz wave equation is deducted from Maxwell equations (2.7) and expected solution (2.8):

$$\mathbf{k} \times [\mathbf{k} \times \mathbf{E}] + \omega^2 \hat{\epsilon} \mathbf{E} = 0, \tag{2.45}$$

and equation for $\mathbf{H}$:

$$\mathbf{H} = \mathbf{N} \times \mathbf{E}, \tag{2.46}$$

where $\mathbf{N} = k_0 \left(\nu_x \mathbf{i} + \nu_y \mathbf{j} + \nu_z \mathbf{k}\right)$.
Equation (2.45) is expanded and assuming isotropic medium ($\hat{\epsilon} = diag\left(\epsilon, \epsilon, \epsilon\right)$) simplified into form:

$$\underbrace{\begin{bmatrix} \epsilon - \nu_y^2 - nu_z^2 & \nu_y\nu_x & \nu_z\nu_x \\ \nu_x\nu_y & \epsilon - \nu_x^2 - \nu_z^2 & \nu_z\nu_y \\ \nu_x\nu_z & \nu_y\nu_z & \epsilon - \nu_x^2 - \nu_y^2 \end{bmatrix}}_{\mathrm{B}} \cdot \begin{bmatrix} \mathbf{e}_x \\ \mathbf{e}_y \\ \mathbf{e}_z \end{bmatrix} = 0 \tag{2.47}$$

Goal of solving (2.47) is to find nontrivial solution for normal component ν_z for ν_x and ν_y given by incident wave. Values ν_z describes propagation direction as well as values in T

matrix, (3.14). Let estimate $\det(\mathrm{B}) = 0$, than ν_z is equal to:

$$\begin{aligned} \nu_{z,1} &= +\sqrt{\epsilon - \nu_x^2 - \nu_y^2} \\ \nu_{z,2} = -\nu_{z,1} &= -\sqrt{\epsilon - \nu_x^2 - \nu_y^2} \\ \nu_{z,3} &= +\sqrt{\epsilon - \nu_x^2 - \nu_y^2} \\ \nu_{z,4} = -\nu_{z,3} &= -\sqrt{\epsilon - \nu_x^2 - \nu_y^2} \end{aligned} \tag{2.48}$$

Propagation constant with positive real part represents down-propagating modes, with negative real part up-propagating modes. This propagation constants are connected with two up- and two down-propagating plane waves. Thus can be chose arbitrary wit limitation of linearly independence. Advantageously they are chosen as a s- and p-polarized waves, however each wave satisfying wave equation (2.47) can be used.

$$\begin{aligned} \mathbf{e}_1 &= \begin{bmatrix} \nu_y \\ -\nu_x \\ 0 \end{bmatrix}, \quad \mathbf{h}_1 = \begin{bmatrix} \nu_x\nu_{z,1} \\ \nu_y\nu_{z,1} \\ -\left(\nu_x^2 + \nu_y^2\right) \end{bmatrix}, \\ \mathbf{e}_2 &= \begin{bmatrix} \nu_y \\ -\nu_x \\ 0 \end{bmatrix}, \quad \mathbf{h}_2 = \begin{bmatrix} -\nu_x\nu_{z,1} \\ \nu_y\nu_{z,1} \\ -\left(\nu_x^2 + \nu_y^2\right) \end{bmatrix}, \\ \mathbf{e}_3 &= \begin{bmatrix} \nu_x\nu_{z,3} \\ \nu_y\nu_{z,3} \\ \left(\nu_x^2 + \nu_y^2\right) \end{bmatrix}, \quad \mathbf{h}_3 = \begin{bmatrix} \nu_y\nu_{z,3}^{-1}\left(\nu_x^2 + \nu_y^2 - \nu_{z,3}^2\right) \\ \nu_x\nu_{z,3}^{-1}\left(\nu_x^2 + \nu_y^2 - \nu_{z,3}^2\right) \\ 0 \end{bmatrix}, \\ \mathbf{e}_4 &= \begin{bmatrix} -\nu_x\nu_{z,3} \\ -\nu_y\nu_{z,3} \\ \left(\nu_x^2 + \nu_y^2\right) \end{bmatrix}, \quad \mathbf{h}_4 = \begin{bmatrix} -\nu_y\nu_{z,3}^{-1}\left(\nu_x^2 + \nu_y^2 - u_{z,3}^2\right) \\ \nu_x\nu_{z,3}^{-1}\left(\nu_x^2 + \nu_y^2 - \nu_{z,3}^2\right) \\ 0 \end{bmatrix}. \end{aligned} \tag{2.49}$$

Realiton (2.46) has been used for calculation magnetic field. Matrix of the tangential components T is assembled from components of field vectors (2.49) according to the column vector $\mathbf{F}$ (2.31) and propagation direction (constant ν_z).

Example 2.4.2
Matrix of tangential component with Yeh approach applied to isotropic homogeneous material
Let the plane of incidence wave be in $y - z$ plane (according to Figure. 3) and isotropic homogeneous medium. Than component of normalized wave vector $\nu_x = 0$, permitivity

tensor $\hat{\epsilon}$ is a diagonal matrix, $\hat{\epsilon} = diag\,(\epsilon, \epsilon, \epsilon)$ and wave equation (2.47) has form:

$$\underbrace{\begin{bmatrix} \epsilon - \nu_y^2 - \nu_z^2 & 0 & 0 \\ 0 & \epsilon - \nu_z^2 & \nu_z\nu_y \\ 0 & \nu_y\nu_z & \epsilon - \nu_y^2 \end{bmatrix}}_{\mathrm{B}} \cdot \begin{bmatrix} \mathbf{e}_x \\ \mathbf{e}_y \\ \mathbf{e}_z \end{bmatrix} = 0 \tag{2.50}$$

From condition $\det(\mathrm{B}) = 0$ are the normal component of refractive index ν_z:

$$\nu_{z,1,3} = \sqrt{\epsilon - \nu_y^2}, \qquad \nu_{z,2,4} = -\sqrt{\epsilon - \nu_y^2} \tag{2.51}$$

Solutions related to values $\nu_{z,i}$ presenting linear polarized waves can be written:

$$\begin{aligned}
\mathbf{e}_1 &= \begin{bmatrix} 1 \\ 0 \\ 0 \end{bmatrix}, & \mathbf{h}_1 &= \begin{bmatrix} 0 \\ \nu_{z,1} \\ -\nu_y \end{bmatrix}, \\
\mathbf{e}_2 &= \begin{bmatrix} 1 \\ 0 \\ 0 \end{bmatrix}, & \mathbf{h}_2 &= \begin{bmatrix} 0 \\ -\nu_{z,1} \\ -\nu_y \end{bmatrix}, \\
\mathbf{e}_3 &= \begin{bmatrix} 0 \\ 0 \\ (\sqrt{\epsilon})^{-1}\sqrt{\epsilon - \nu_y^2} \\ -\sqrt{\epsilon}\nu_y \end{bmatrix}, & \mathbf{h}_3 &= \begin{bmatrix} -\sqrt{\epsilon} \\ 0 \\ 0 \end{bmatrix}, \\
\mathbf{e}_4 &= \begin{bmatrix} 0 \\ 0 \\ (\sqrt{\epsilon})^{-1}\sqrt{\epsilon - \nu_y^2} \\ \sqrt{\epsilon}\nu_y \end{bmatrix}, & \mathbf{h}_4 &= \begin{bmatrix} \sqrt{\epsilon} \\ 0 \\ 0 \end{bmatrix}.
\end{aligned} \tag{2.52}$$

Separating tangential components of $\mathbf{e}$ and $\mathbf{h}$ is assembled matrix T_{iso}. Columns of matrix are ordered with respect to related propagation constants, normal components of refractive index $\nu_{z,i}$. According to system of coordinates and convention (2.12) has down-propagating wave positive real part of $\nu_{z,i}$ and up-propagating mode negative real part. Using the same ordering as in Example. 2.4.1 and (2.44), is the tangential component matrix:

$$\mathrm{T}_{iso} = \begin{bmatrix} 1 & 1 & 0 & 0 \\ \sqrt{\epsilon - \nu_y^2} & -\sqrt{\epsilon - \nu_y^2} & 0 & 0 \\ 0 & 0 & (\sqrt{\epsilon})^{-1}\sqrt{\epsilon - \nu_y^2} & (\sqrt{\epsilon})^{-1}\sqrt{\epsilon - \nu_y^2} \\ 0 & 0 & -\sqrt{\epsilon} & \sqrt{\epsilon} \end{bmatrix}, \tag{2.53}$$

and matrix of propagation constant:

$$\mathrm{V}_{iso} = \begin{bmatrix} \sqrt{\epsilon - \nu_y^2} & 0 & 0 & 0 \\ 0 & -\sqrt{\epsilon - \nu_y^2} & 0 & 0 \\ 0 & 0 & \sqrt{\epsilon - \nu_y^2} & 0 \\ 0 & 0 & 0 & -\sqrt{\epsilon - \nu_y^2} \end{bmatrix}, \tag{2.54}$$

It is easy to see that two different approaches, Berreman's and Yeh's formalism, has the same result in form of the tangential components matrices and the propagation constant matrices. ■

2.5 Boundary conditions for planar interface

In this section theoretical results about solving Maxwell equations in medium based on tangential components continuity (Chapter 2.4.) is applied to planar layers system. Firstly is discussed case with one layer (see Figure 5.) surrounded with substrate and superstrate. System contains two interfaces and is necessary cover up propagation thought layer. Eigenmodes of ellipticaly polarized electromagnetic wave in i-th medium are represented by $\mathrm{C}^{(i)}$ matrix eigenvectors.

$$\begin{array}{l} \mathrm{T}^{(i)}\mathbf{A}^{(i)}\left(z_i\right) \\ \hline \mathrm{T}^{(i+1)}\mathbf{A}^{(i+1)}\left(z_i\right) \end{array} \quad (z_i)$$

$$\mathrm{P}^{(i+1)}$$

$$\begin{array}{l} \mathrm{T}^{(i+1)}\mathbf{A}^{(i+1)}\left(z_{i+1}\right) \\ \hline \mathrm{T}^{(i+2)}\mathbf{A}^{(i+2)}\left(z_{i+1}\right) \end{array} \quad z_{(i+1)}$$

Figure 5: Wave transformation in propagation across from one layer

Analytical formulas for isotropic homogeneous medium is derived in Example 2.4.1. Let us to define vector of amplitudes $\mathbf{A}^{(i)}$:

$$\mathbf{A}^{(i)} = \left[A^{(i)}_{1_{down}}, A^{(i)}_{2_{up}}, A^{(i)}_{3_{down}}, A^{(i)}_{4_{up}}\right]^T \tag{2.55}$$

because columns of eigenmodes matrix $\mathrm{T}^{(i)_{iso}}$ (2.43) has the same ordering. Matrix $\mathrm{T}^{(i+1)}$ is easy to calculate from $\mathrm{C}^{(i+1)}$ (2.36). Followed equation results from tangential components continuity:

$$\mathrm{T}^{(i)}\mathbf{A}^{(i)}\left(z_i\right) = \mathrm{T}^{(i+1)}\mathbf{A}^{(i+1)}\left(z_i\right). \tag{2.56}$$

Now it is easy to give an expression of amplitudes on the other interface side:

$$\mathbf{A}^{(i)}\left(z_i\right) = \left(\mathrm{T}^{(i)}\right)^{-1}\mathrm{T}^{(i+1)}\mathbf{A}^{(i+1)}\left(z_i\right). \tag{2.57}$$

Amplitudes change at the lower interface (z_{i+1}) is in the same relation:

$$\mathbf{A}^{(i+1)}\left(z_{i+1}\right) = \left(\mathrm{T}^{(i+1)}\right)^{-1}\mathrm{T}^{(i+2)}\mathbf{A}^{(i+2)}\left(z_{i+1}\right). \tag{2.58}$$

Propagating wave through layer from interface (z_i) to (z_{i+1}) is changed and this effect is described with propagation matrix $\mathrm{P}^{(i)}$:

$$\mathrm{P}^{(i)} = \begin{bmatrix} \exp\left(\mathrm{i}k_0 \left[\mathrm{V}\right]_{1,1} d^{(i)}\right) & 0 & 0 & 0 \\ 0 & \exp\left(\mathrm{i}k_0 \left[\mathrm{V}\right]_{2,2} d^{(i)}\right) & 0 & 0 \\ 0 & 0 & \exp\left(\mathrm{i}k_0 \left[\mathrm{V}\right]_{3,3} d^{(i)}\right) & 0 \\ 0 & 0 & 0 & \exp\left(\mathrm{i}k_0 \left[\mathrm{V}\right]_{4,4} d^{(i)}\right) \end{bmatrix}, \tag{2.59}$$

where $[\mathrm{V}]_{ii}$ are propagation constants, d_i is the thickness of i-th layer and the vector of amplitudes is transformed according to relation:

$$\mathbf{A}^{(i+1)}\left(z_{i+1}\right) = \mathrm{P}^{(i)}\mathbf{A}^{(i+1)}\left(z_i\right). \tag{2.60}$$

Relation between wave in superstrate $\mathbf{A}^{(i)}\left(z_i\right)$ and wave in substrate $\mathbf{A}^{(i+2)}\left(z_{i+1}\right)$ is given by combination (2.56-2.60):

$$\mathbf{A}^{(i)}\left(z_i\right) = \left(\mathrm{T}^{(i)}\right)^{-1} \mathrm{T}^{(i+1)} \left(\mathrm{P}^{(i+1)}\right)^{-1} \left(\mathrm{T}^{(i+1)}\right)^{-1} \mathrm{T}^{(i+2)}\mathbf{A}^{(i+2)}\left(z_{i+1}\right). \tag{2.61}$$

For system with N planar layers is relation between vector of amplitudes in superstrate and substrate following form[1]:

$$\mathbf{A}^{(0)} = \left(\mathrm{T}^{(0)}\right)^{-1} \left(\prod_{i=1}^{N} \mathrm{T}^{(i)} \left(\mathrm{P}^{(i)}\right)^{-1} \left(\mathrm{T}^{(i)}\right)^{-1}\right) \mathrm{T}^{(N+1)}\mathbf{A}^{(N+1)} = \mathrm{M}\mathbf{A}^{(N+1)}. \tag{2.62}$$

In each point of layer can exists four independent modes, $\mathbf{F}^{(i)}_{up}, \mathbf{F}^{(i)}_{down}, \mathbf{F}^{(i)}_{up}, \mathbf{F}^{(i)}_{down}$. Considering C of general material (anisotropic, homogeneous), eigenvectors matrix T can be written:

$$\mathrm{T}^{(i)} = \begin{bmatrix} \mathbf{e}^{(i)}_{1,x} & \mathbf{e}^{(i)}_{2,x} & \mathbf{e}^{(i)}_{3,x} & \mathbf{e}^{(i)}_{4,x} \\ \mathbf{h}^{(i)}_{1,y} & \mathbf{h}^{(i)}_{2,y} & \mathbf{h}^{(i)}_{3,y} & \mathbf{h}^{(i)}_{4,y} \\ \mathbf{e}^{(i)}_{1,y} & \mathbf{e}^{(i)}_{2,y} & \mathbf{e}^{(i)}_{3,y} & \mathbf{e}^{(i)}_{4,y} \\ \mathbf{h}^{(i)}_{1,x} & \mathbf{h}^{(i)}_{2,x} & \mathbf{h}^{(i)}_{3,x} & \mathbf{h}^{(i)}_{4,x} \end{bmatrix}. \tag{2.63}$$

For each wave in structure is defined amplitudes vector $\mathbf{A}^{(i)} = \left[A^{(i)}_{1_{down}}, A^{(i)}_{2_{up}}, A^{(i)}_{3_{down}}, A^{(i)}_{4_{up}}\right]^T$. Product of $\mathrm{T}^{(i)}\mathbf{A}^{(i)}$ is total values of tangential field components at various point of structure:

$$\underbrace{\begin{bmatrix} \mathbf{e}_{1,x} & \mathbf{e}_{2,x} & \mathbf{e}_{3,x} & \mathbf{e}_{4,x} \\ \mathbf{h}_{1,y} & \mathbf{h}_{2,y} & \mathbf{h}_{3,y} & \mathbf{h}_{4,y} \\ \mathbf{e}_{1,y} & \mathbf{e}_{2,y} & \mathbf{e}_{3,y} & \mathbf{e}_{4,y} \\ \mathbf{h}_{1,x} & \mathbf{h}_{2,x} & \mathbf{h}_{3,x} & \mathbf{h}_{4,x} \end{bmatrix}}_{\mathrm{T}} \begin{bmatrix} A_{1_{down}} \\ A_{2_{up}} \\ A_{3_{down}} \\ A_{4_{up}} \end{bmatrix} = \begin{bmatrix} \mathbf{e}_x \\ \mathbf{h}_y \\ \mathbf{e}_y \\ \mathbf{h}_x \end{bmatrix}. \tag{2.64}$$

[1] It is not necessary to calculate inversion to matrix $\mathrm{P}^{(i)}$ in numerical implementation, changing the sign in exponential factor spends calculation time.

2.5.1 Reflection coefficients

In case of isotropic medium, the eigenmodes are linearly *s*- and *p*-polarized waves. Reflection coefficients of *s*- and *p*-polarized wave can be expressed from relation (2.62) and amplitude vector definition (2.55). Components of amplitudes vectors are partially set down from character of physical problem: incidence wave from superstrat $\mathbf{A}_1^{(0)} = 1$, $(\mathbf{A}_3^{(0)} = 1)$ for *s*- (or *p*-) polarized wave and no incoming wave from substrat $\mathbf{A}_2^{(N)} = \mathbf{A}_2^{(N)} = 0$. Remaining components of amplitude vector can be computed from reflection coefficients:

$$\begin{aligned} r_{ss} &= \frac{\mathrm{M}_{21}\mathrm{M}_{33} - \mathrm{M}_{23}\mathrm{M}_{31}}{\mathrm{M}_{11}\mathrm{M}_{33} - \mathrm{M}_{13}\mathrm{M}_{31}} \\ r_{sp} &= \frac{\mathrm{M}_{41}\mathrm{M}_{33} - \mathrm{M}_{43}\mathrm{M}_{31}}{\mathrm{M}_{11}\mathrm{M}_{33} - \mathrm{M}_{13}\mathrm{M}_{31}} \\ r_{ps} &= \frac{\mathrm{M}_{11}\mathrm{M}_{23} - \mathrm{M}_{21}\mathrm{M}_{13}}{\mathrm{M}_{11}\mathrm{M}_{33} - \mathrm{M}_{13}\mathrm{M}_{31}} \\ r_{pp} &= \frac{\mathrm{M}_{11}\mathrm{M}_{43} - \mathrm{M}_{41}\mathrm{M}_{13}}{\mathrm{M}_{11}\mathrm{M}_{33} - \mathrm{M}_{13}\mathrm{M}_{31}} \end{aligned} \tag{2.65}$$

2.6 Numerical model: surface plasmon resonance on gold layer

Plasmon resonances in nanostructures are very promissing to locally enhance electromagnetic field in the structure and new phenomena are observed. A new phenomena of ”plasmons” and ”magnetopalasmons” is in the focus of recent research. In this subsection the surface plasmon in Au-wather interface is modeled. Figure 6. demonstrates system of the glass prism with gold layer and water as substrate. For proper configuration of the angle of incidence in glass, the wavelength, thickness of gold layer and *p*-polarized light the plasnom plasmon resonance can be excited on gold layer.

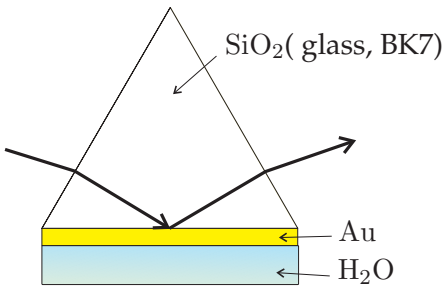

Figure 6: Configuration for Surface plasmon resonance with glass prism and gold layer.

Parameters used in model:

- wavelength: 589.3 nm
- thick of Au film: 44nm
- refractive index of glass: $1,515$
- refractive index of gold: $0.28 + 3.017$i
- refractive index of water: $1,33$

Figure 7. shows schematically the glass superstrate, the planar gold layer and water as substrate.

$\mathrm{T}^{\mathrm{SiO_2}}\mathbf{A}^{\mathrm{SiO_2}}$	$\mathrm{SiO_2}$
$\mathrm{T}^{\mathrm{Au}}\mathbf{A}^{\mathrm{Au}}$	Au
$\mathrm{T}^{\mathrm{H_2O}}\mathbf{A}^{\mathrm{H_2O}}$	$\mathrm{H_2O}$

Figure 7: System of planar layers in SPR system

According to M-matrix algorithm (2.62) is assembled the M-matrix of the system for angles of incidence $\phi \in (0, 90)$. For each angle of incidence is calculated the M-matrix and the reflectance coefficients $R_S = r_{ss}r^*_{ss}$ and $R_p = r_{pp}r^*_{pp}$, (see eq. 2.65):

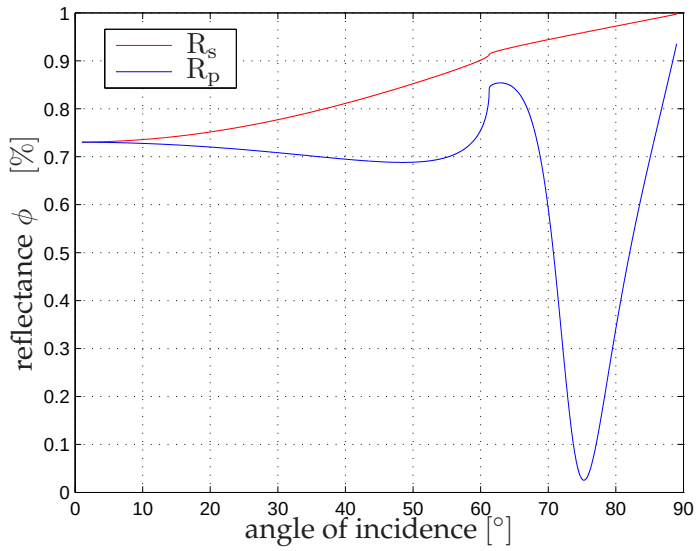

Figure 8: Dependence of the reflectance on angle of incidence for system glass-gold-water.

From Figure 8. we can see the plasmon excitation for the angle of incidence $\phi = 74.8°$. As expected, the surface plasmon resonance is observed onlz for *p*-polarized wave.

3 Polarized light in periodical structures

3.1 One-dimensional grating

One dimensional grating consists of periodical lamellar structure. System of planar layers presented in previous chapter can be considered as a zero-dimension problem because there is no periodical medium. Other point of view is that planar layer is periodical structure made of two same materials with the infinite period Λ. Usual one-dimensional grating is shown on Figure 9. In following calculations let's consider the plane of incidence in $y - z$ plane,

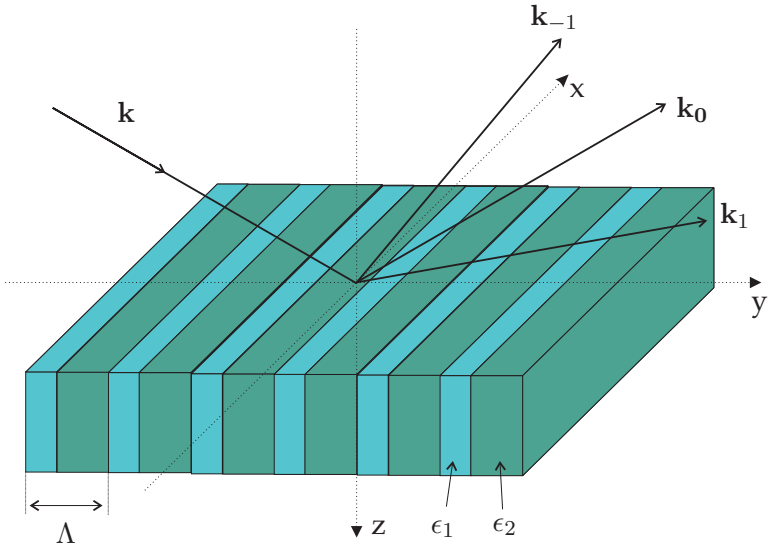

Figure 9: System of coordinates for 1D grating

the plane of incidence is perpendicular to lamellas. Because gratings permitivity tensor is a discontinuous function it is necessary to use more advanced method for calculating with field tangential components instead of M-matrix algorithm (2.62) in planar layers. Algorithm discussed in this work is Rigorous Coupled Wave Analysis (RCWA) based on approximation of permitivity function by its truncated Fourier series [12].

3.1.1 RCWA algorithm for periodic structures

Equations describing field in the structure are the same normalized Maxwell equations as defined in Chapter 2.4 (2.25):

$$\nabla \times \mathbf{H}'(\mathbf{r}) = -\mathrm{i}k_0 \hat{\epsilon} \mathbf{E}'(\mathbf{r}), \tag{3.1a}$$

$$\nabla \times \mathbf{E}'(\mathbf{r}, t) = \mathrm{i}k_0 \mathbf{H}'(\mathbf{r}). \tag{3.1b}$$

Difference is that the permitivity tensor $\hat{\epsilon}$ is now function of y axis direction. For that can be elements ϵ_{ij} expanded into its Fourier series (see Example 3.1.2.):

$$\epsilon_{ij}(\mathbf{r}) = \sum_{n=-\infty}^{\infty} \epsilon_{ij,n} \exp\left(\mathrm{i}n\frac{2\pi}{\Lambda}y\right), \tag{3.2}$$

where Λ is period of gratings lammelas and $\epsilon_{ij,n}$ is n-th Fourier series coefficient defined[2].:

$$\epsilon_{ij,n} = \frac{1}{\Lambda}\int_0^{\Lambda} \epsilon_{ij}(y)\exp\left(-\mathrm{i}n\frac{2\pi}{\Lambda}y\right)dy. \tag{3.3}$$

Same expansion is applied to electric and magnetic field vectors $\mathbf{E}^{'}, \mathbf{H}^{'}$ in every layer in medium including homogeneous layers. In superstrate the expansion has meaning of all possible incident a reflected waves. In substrate expansion leads to description of all propagated modes through medium. Because the x and y components of wave vector does not change in each layer, they can be described in the form:

$$\mathbf{E}^{'}(\mathbf{r}) = \sum_{n=-\infty}^{\infty} E_{0,n}\mathbf{e}_n(z)\exp\left(\mathrm{i}k_0\left(\nu_x x + \nu_y y\right)\right)\exp\left(\mathrm{i}n\frac{2\pi}{\Lambda}y\right), \tag{3.4a}$$

$$\mathbf{H}^{'}(\mathbf{r}) = \sum_{n=-\infty}^{\infty} H_{0,n}\mathbf{h}_n(z)\exp\left(\mathrm{i}k_0\left(\nu_x x + \nu_y y\right)\right)\exp\left(\mathrm{i}n\frac{2\pi}{\Lambda}y\right). \tag{3.4b}$$

In computing is not possible to calculate with infinite Fourier expansion. For that is expansion symmetrically truncated to $2N+1$ diffraction orders. Using equations (3.4a) and (3.4b) in Maxwell equation (2.25a) and (2.25b) can be written in form:

$$\nabla \times \sum_{n=-N}^{N} \mathbf{h}_n \exp\left(\mathrm{i}k_0\left(\nu_x x + \nu_y y\right)\right)\exp\left(\mathrm{i}n\frac{2\pi}{\Lambda}y\right) =$$

$$-\mathrm{i}k_0 \sum_{n=-N}^{N}\sum_{m=-N}^{N} \hat{\epsilon}_{n-m}\mathbf{e}_n \exp\left(\mathrm{i}k_0\left(\nu_x x + \nu_y y\right)\right)\exp\left(\mathrm{i}n\frac{2\pi}{\Lambda}y\right), \tag{3.5}$$

$$\nabla \times \sum_{n=-N}^{N} \mathbf{e}_n \exp\left(\mathrm{i}k_0\left(\nu_x x + \nu_y y\right)\right)\exp\left(\mathrm{i}n\frac{2\pi}{\Lambda}y\right) =$$

$$\mathrm{i}k_0 \sum_{n=-N}^{N} \mathbf{h}_n \exp\left(\mathrm{i}k_0\left(\nu_x x + \nu_y y\right)\right)\exp\left(\mathrm{i}n\frac{2\pi}{\Lambda}y\right), \tag{3.6}$$

where $\hat{\epsilon}_n$ is tensor of n-th truncated Fourier expansion components. Compact form of (3.5) and (3.6) is better for further calculation and implementation:

$$\nabla \times \left\{\mathrm{F}\left\lceil \mathbf{h}(z)\right\rceil \exp\left(\mathrm{i}k_0\left(\nu_x x + \nu_y y\right)\right)\right\} = -\mathrm{i}k_0 \mathrm{F}\left\lceil\!\left\lceil \hat{\epsilon}\right\rceil\!\right\rceil \left\lceil \mathbf{e}(z)\right\rceil \exp\left(\mathrm{i}k_0\left(k_x x + k_y y\right)\right), \tag{3.7a}$$

$$\nabla \times \left\{\mathrm{F}\left\lceil \mathbf{e}(z)\right\rceil \exp\left(\mathrm{i}k_0\left(\nu_x x + \nu_y y\right)\right)\right\} = \mathrm{F}\left\lceil \mathbf{h}(z)\right\rceil \exp\left(\mathrm{i}k_0\left(\nu_x x + \nu_y y\right)\right), \tag{3.7b}$$

Matrix F is a matrix with Fourier exponents on its diagonal and has size $(2N+1)\times(2N+1)$:

$$F_{ij} = \delta_{ij}\exp\left(\mathrm{i}\left(j - N - 1\right)\frac{2\pi}{\Lambda}\right). \tag{3.8}$$

The symbol $\lceil . \rceil$ stands by the amplitudes vector of truncated Fourier expansion (in the y direction) and symbol $\lceil\!\lceil . \rceil\!\rceil$ stands by Toeplitz amplitude matrix of expanded permitivity

[2]In general case grating layer can be made of more than two materials

tensor function $\hat{\epsilon}(y)$ (see Example 3.1.1.). Before transforming equations in the same way like in (2.26) are both sides multiplied with F^{-1} and equations are particularly derived with respect to constant tangential components (much like in (2.28))

$$\begin{bmatrix} 0 & 0 & 0 & 0 & -\frac{\partial}{\partial z} & \frac{\partial}{\partial y} \\ 0 & 0 & 0 & \frac{\partial}{\partial z} & 0 & -\frac{\partial}{\partial x} \\ 0 & 0 & 0 & -\frac{\partial}{\partial y} & \frac{\partial}{\partial x} & 0 \\ 0 & -\frac{\partial}{\partial z} & \frac{\partial}{\partial y} & 0 & 0 & 0 \\ \frac{\partial}{\partial z} & 0 & -\frac{\partial}{\partial x} & 0 & 0 & 0 \\ -\frac{\partial}{\partial y} & \frac{\partial}{\partial x} & 0 & 0 & 0 & 0 \end{bmatrix} \begin{bmatrix} \lceil \mathbf{e}_x(\mathbf{r}) \rceil \\ \lceil \mathbf{e}_y(\mathbf{r}) \rceil \\ \lceil \mathbf{e}_z(\mathbf{r}) \rceil \\ \lceil \mathbf{h}_x(\mathbf{r}) \rceil \\ \lceil \mathbf{h}_y(\mathbf{r}) \rceil \\ \lceil \mathbf{h}_z(\mathbf{r}) \rceil \end{bmatrix} =$$

$$= ik_0 \begin{bmatrix} -\epsilon_{xx} & -\epsilon_{xy} & -\epsilon_{xz} & 0 & 0 & 0 \\ -\epsilon_{yx} & -\epsilon_{yy} & -\epsilon_{yz} & 0 & 0 & 0 \\ -\epsilon_{zx} & -\epsilon_{zy} & -\epsilon_{zz} & 0 & 0 & 0 \\ 0 & 0 & 0 & 1 & 0 & 0 \\ 0 & 0 & 0 & 0 & 1 & 0 \\ 0 & 0 & 0 & 0 & 0 & 1 \end{bmatrix} \begin{bmatrix} \lceil \mathbf{e}_x(\mathbf{r}) \rceil \\ \lceil \mathbf{e}_y(\mathbf{r}) \rceil \\ \lceil \mathbf{e}_z(\mathbf{r}) \rceil \\ \lceil \mathbf{h}_x(\mathbf{r}) \rceil \\ \lceil \mathbf{h}_y(\mathbf{r}) \rceil \\ \lceil \mathbf{h}_z(\mathbf{r}) \rceil \end{bmatrix}. \tag{3.9}$$

And after derivation:

$$\begin{bmatrix} 0 & 0 & 0 & 0 & -\frac{\partial}{\partial z} & \mathrm{i}k_0\mathrm{q} \\ 0 & 0 & 0 & \frac{\partial}{\partial z} & 0 & -\mathrm{i}k_0\mathrm{p} \\ 0 & 0 & 0 & -\mathrm{i}k_0\mathrm{q} & \mathrm{i}k_0\mathrm{p} & 0 \\ 0 & -\frac{\partial}{\partial z} & \mathrm{i}k_0\mathrm{q} & 0 & 0 & 0 \\ \frac{\partial}{\partial z} & 0 & -\mathrm{i}k_0\mathrm{p} & 0 & 0 & 0 \\ -\mathrm{i}k_0\mathrm{q} & \mathrm{i}k_0\mathrm{p} & 0 & 0 & 0 & 0 \end{bmatrix} \begin{bmatrix} \lceil \mathbf{e}_x(\mathbf{r}) \rceil \\ \lceil \mathbf{e}_y(\mathbf{r}) \rceil \\ \lceil \mathbf{e}_z(\mathbf{r}) \rceil \\ \lceil \mathbf{h}_x(\mathbf{r}) \rceil \\ \lceil \mathbf{h}_y(\mathbf{r}) \rceil \\ \lceil \mathbf{h}_z(\mathbf{r}) \rceil \end{bmatrix} =$$

$$= \mathrm{i}k_0 \begin{bmatrix} -\epsilon_{xx} & -\epsilon_{xy} & -\epsilon_{xz} & 0 & 0 & 0 \\ -\epsilon_{yx} & -\epsilon_{yy} & -\epsilon_{yz} & 0 & 0 & 0 \\ -\epsilon_{zx} & -\epsilon_{zy} & -\epsilon_{zz} & 0 & 0 & 0 \\ 0 & 0 & 0 & 1 & 0 & 0 \\ 0 & 0 & 0 & 0 & 1 & 0 \\ 0 & 0 & 0 & 0 & 0 & 1 \end{bmatrix} \begin{bmatrix} \lceil \mathbf{e}_x(\mathbf{r}) \rceil \\ \lceil \mathbf{e}_y(\mathbf{r}) \rceil \\ \lceil \mathbf{e}_z(\mathbf{r}) \rceil \\ \lceil \mathbf{h}_x(\mathbf{r}) \rceil \\ \lceil \mathbf{h}_y(\mathbf{r}) \rceil \\ \lceil \mathbf{h}_z(\mathbf{r}) \rceil \end{bmatrix}. \tag{3.10}$$

The matrices p and q are diagonal with elements representing tangential component of normalized wave vector, $p_{ij} = \delta_{i,j}\nu_x$ and $q_{ij} = \delta_{ij}\left(\nu_y + (j - N - 1)\frac{\lambda}{\Lambda}\right)$, for $i, j \in \{1, 2, \ldots, 2N+1\}$. From the equation (3.10) can be separated normal component and

expressed with tangential components in the same meaning as in (2.30-2.34). Finally after some calculation the vector of tangential components is defined :

$$\lceil \mathbf{F}(z) \rceil = \left[\left\lceil e'_x(z) \right\rceil, \left\lceil h'_y(z) \right\rceil, \left\lceil e'_y(z) \right\rceil, \left\lceil h'_x(z) \right\rceil \right]^T, \tag{3.11}$$

and the same type of eigenvalue problem:

$$\frac{\partial}{\partial z} \lceil \mathbf{F}(z) \rceil = \mathrm{i}k_0 \mathrm{C} \lceil \mathbf{F}(z) \rceil. \tag{3.12}$$

The size of the matrix C is now $4(2N+1) \times 4(2N+1)$ and has the following form:

$$\begin{bmatrix}
-\mathrm{p} \left[\!\left[\varepsilon_{zz}^{-1} \right]\!\right] [\![\varepsilon_{zx}]\!] & \mathbb{I} - \mathrm{p} \left[\!\left[\varepsilon_{zz}^{-1} \right]\!\right] & \vdots \\
-\mathrm{q}^2 + [\![\varepsilon_{xx}]\!] - [\![\varepsilon_{xz}]\!] \left[\!\left[\varepsilon_{zz}^{-1} \right]\!\right] [\![\varepsilon_{zx}]\!] & - [\![\varepsilon_{xz}]\!] \left[\!\left[\varepsilon_{zz}^{-1} \right]\!\right] \mathrm{p} & \vdots \\
-\mathrm{q} \left[\!\left[\varepsilon_{zz}^{-1} \right]\!\right] [\![\varepsilon_{zx}]\!] & -\mathrm{q} \left[\!\left[\varepsilon_{zz}^{-1} \right]\!\right] \mathrm{p} & \vdots \\
\mathrm{pq} - [\![\varepsilon_{yx}]\!] + [\![\varepsilon_{yz}]\!] \left[\!\left[\varepsilon_{zz}^{-1} \right]\!\right] [\![\varepsilon_{zx}]\!] & [\![\varepsilon_{yz}]\!] \left[\!\left[\varepsilon_{zz}^{-1} \right]\!\right] \mathrm{p} & \vdots \\
\vdots & -\mathrm{p} \left[\!\left[\varepsilon_{zz}^{-1} \right]\!\right] [\![\varepsilon_{zy}]\!] & \mathrm{p} \left[\!\left[\varepsilon_{zz}^{-1} \right]\!\right] \mathrm{q} \\
\vdots & \mathrm{qp} + [\![\varepsilon_{xy}]\!] - [\![\varepsilon_{xz}]\!] \left[\!\left[\varepsilon_{zz}^{-1} \right]\!\right] [\![\varepsilon_{zy}]\!] & [\![\varepsilon_{xz}]\!] \left[\!\left[\varepsilon_{zz}^{-1} \right]\!\right] \mathrm{q} \\
\vdots & -\mathrm{q} \left[\!\left[\varepsilon_{zz}^{-1} \right]\!\right] [\![\varepsilon_{zy}]\!] & \mathrm{q} \left[\!\left[\varepsilon_{zz}^{-1} \right]\!\right] \mathrm{q} - \mathbb{I} \\
\vdots & \mathrm{p}^2 - [\![\varepsilon_{yy}]\!] + [\![\varepsilon_{yz}]\!] \left[\!\left[\varepsilon_{zz}^{-1} \right]\!\right] [\![\varepsilon_{zy}]\!] & - [\![\varepsilon_{yz}]\!] \left[\!\left[\varepsilon_{zz}^{-1} \right]\!\right] \mathrm{q}
\end{bmatrix} \tag{3.13}$$

Again is result system of first degree differential equations with constant coefficients and the solution $\mathbf{g}(z)$ can be written:

$$\lceil \mathbf{g}(z) \rceil = \exp(\mathrm{i}k_0 z_i \mathrm{V}) \mathbf{A}, \tag{3.14}$$

where $\mathbf{A}$ is the vector of amplitudes of each wave mode.

Example 3.1.1
Toeplitz matrix of permitivity tensor function
In general Toeplitz matrix A has the following form:

$$\mathrm{A} = \begin{bmatrix}
a_0 & a_{-1} & a_{-2} & \dots & \dots & a_{-n+1} \\
a_1 & a_0 & a_{-1} & \ddots & & \vdots \\
a_2 & a_1 & \ddots & \ddots & \ddots & \vdots \\
\vdots & \ddots & \ddots & \ddots & a_{-1} & a_{-2} \\
\vdots & & \ddots & a_1 & a_0 & a_{-1} \\
a_{n-1} & \dots & \dots & a_2 & a_1 & a_0
\end{bmatrix} \tag{3.15}$$

Let the permitivity tensor is a piecewise constant function:

$$\hat{\epsilon}\left(y\right)=\begin{cases}\hat{\epsilon}_1 & \text{for} \quad y\in\langle 0,y_1)\\ \hat{\epsilon}_2 & \vdots \quad y\in\langle y_1,y_2)\\ \vdots & \vdots \quad \vdots\\ \hat{\epsilon}_n & \text{for} \quad y\in\langle y_{n-1},\Lambda\rangle\end{cases} \tag{3.16}$$

where $\hat{\epsilon}_i, \quad i\in\{1,2,\cdots,n\}$ is 3×3 matrix (2.15). Lets consider Fourier approximation only for $\epsilon_{xx}\left(y\right)$ component and number of diffraction orders $N=1$. Recipe of constructing symmetrical Fourier approximation (3.3) gives five amplitude constants $[\epsilon_{xx,-2},\epsilon_{xx,-1},\epsilon_{xx,0},\epsilon_{xx,1},\epsilon_{xx,2}]$. Toeplitz matrix approximating permitivity function $\epsilon_{xx}\left(y\right)$ has form:

$$\left[\!\left[\epsilon_{xx}\right]\!\right]=\begin{bmatrix}\epsilon_{xx,0} & \epsilon_{xx,-1} & \epsilon_{xx,-2}\\ \epsilon_{xx,1} & \epsilon_{xx,0} & \epsilon_{xx,-1}\\ \epsilon_{xx,2} & \epsilon_{xx,1} & \epsilon_{xx,0}\end{bmatrix} \tag{3.17}$$

■

Example 3.1.2
Truncated Fourier series approximation
Truncation of Fourier series bring an error into truly function of permitivity. For that truncation is appropriate to have an idea about difference between real function $\hat{\epsilon}\left(y\right)$ and its approximation $\hat{\tilde{\epsilon}}\left(y\right)$. For simplicity it was chosen isotropic material with diagonal permitivity $\epsilon_{ij}=\delta_{ij}\epsilon\left(y\right)$ defined:

$$\hat{\epsilon}\left(y\right)=\begin{cases}1 & \text{for} \quad y\in\langle 0,10\text{e}-9)\\ 4 & \quad y\in\langle 10\text{e}-9,30\text{e}-9\rangle\end{cases}, \tag{3.18}$$

period of grating $\Lambda=30nm$. Figure 10. shows effect of truncation of the series (3.2) for the piece wise function (3.18).

■

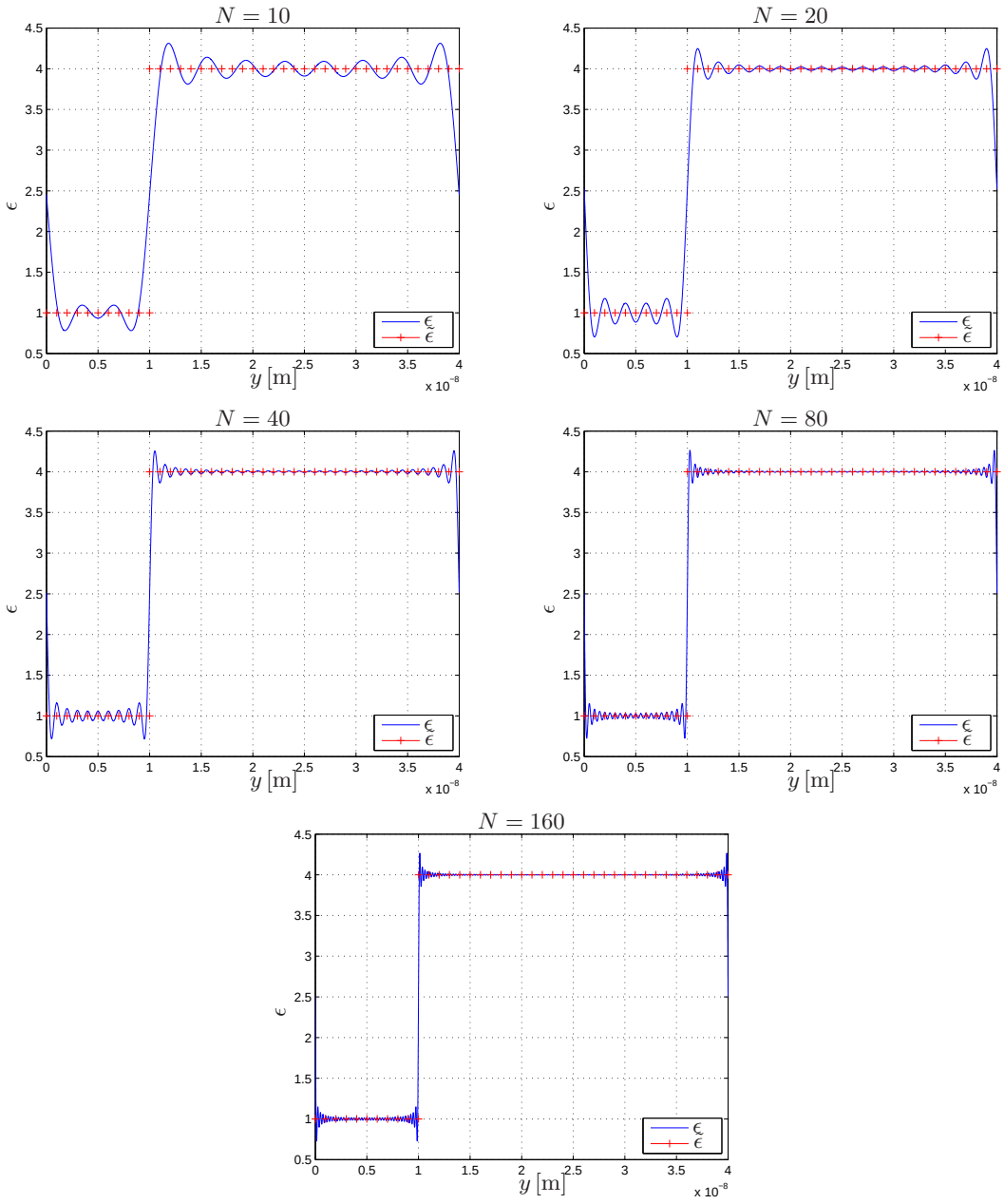

Figure 10: The quality of truncated Fourier series approximation for number of diffraction orders $N = \{10, 20, 40, 80, 160\}$.

3.1.2 S-matrix algorithm

Using the M-matrix algorithm presented in Section 2.5, (2.62) does not work for gratings. Problem is with finite precision of numerical calculation, because introduction of diffraction orders and Fourier amplitudes coefficient causes that arguments of exponential function are higher for higher diffraction orders and the computing sooner or later exceeds numerical precision. Idea of S-matrix algorithm is separation of *up* and *down* modes and calcu-

lation propagation of highly exponentially increasing function of higher diffraction orders in opposite direction which modify exponential factors. Figure 11. shows different calcu-

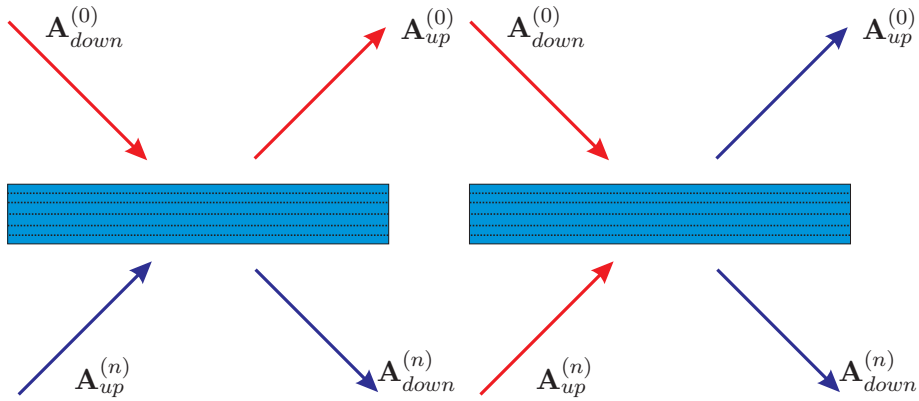

Figure 11: Differences between input (red) and output (blue) arguments in M-matrix and S-matrix algorithms

lation approach in M-matrix and S-matrix algorithm. M-matrix calculate transformations of amplitude vector during propagation medium from superstrate to substrate in contrast with S-matrix algorithm describing relations between waves incoming and outcoming from medium. Following calculations shows basic steps of the S-matrix algorithm. First step is separation of *up* and *down* modes:

$$\begin{array}{cccc} \uparrow & \mathbf{A}^{(i)}_{up} & \downarrow & \mathbf{A}^{(i)}_{down} \\ \hline \uparrow & \mathbf{A}^{(i+1)}_{up} & \downarrow & \mathbf{A}^{(i+1)}_{down} \\ \hline \uparrow & \mathbf{A}^{(i+2)}_{up} & \downarrow & \mathbf{A}^{(i+2)}_{down} \end{array} \begin{array}{l} (z_i) \\ \\ (z_{i+1}) \end{array}$$

Figure 12: Separated *up* and *down* propagating modes in medium

From continuity of field tangential components are the amplitudes $\mathbf{A}^{(i)}(z_i)$ and $\mathbf{A}^{(i+1)}(z_i)$ in relation (2.57):

$$\mathbf{A}^{(i)}(z_i) = \underbrace{\left(\mathrm{T}^{(i)}\right)^{-1}\mathrm{T}^{(i+1)}}_{\mathrm{M}}\mathbf{A}^{(i+1)}(z_i), \tag{3.19}$$

next step is separate *up* and *down* modes:

$$\begin{bmatrix} \mathbf{A}^{(i)}_{up} \\ \mathbf{A}^{(i)}_{down} \end{bmatrix} = \begin{bmatrix} M^{(i)}_{11} & M^{(i)}_{12} \\ M^{(i)}_{21} & M^{(i)}_{22} \end{bmatrix} \begin{bmatrix} \mathbf{A}^{(i+1)}_{up} \\ \mathbf{A}^{(i+1)}_{down} \end{bmatrix}. \tag{3.20}$$

This continuity equation with M is now reorganized into s-matrix form, which keep conti-

nuity too:

$$\begin{bmatrix} \mathbf{A}_{up}^{(i)} \\ \mathbf{A}_{down}^{(i+1)} \end{bmatrix} = s^{(i)} \begin{bmatrix} \mathbf{A}_{up}^{(i+1)} \\ \mathbf{A}_{down}^{(i)} \end{bmatrix}, \tag{3.21}$$

where matrix $\mathrm{s}^{(i)}$ comes from M matrix:

$$\mathrm{s}^{(i)} = \begin{bmatrix} s_{11}^{(i)} & s_{12}^{(i)} \\ s_{21}^{(i)} & s_{22}^{(i)} \end{bmatrix} = \begin{bmatrix} M_{11}^{(i)} - M_{12}{}^{(i)} M_{22}^{(i)-1} M_{21}^{(i)} & M_{12}^{(i)} M_{22}^{(i)-1} \\ M_{22}^{(i)-1} M_{21}^{(i)} & M_{22}^{(i)-1} \end{bmatrix}. \tag{3.22}$$

Now is description of the amplitudes changes on the interface clear and next step is the description of the wave propagation through layer with the propagation matrix $\mathrm{P}^{(i)}$ according to (2.60). The propagation matrix can be also written separately for *up* and *down* modes:

$$\mathbf{A}_{up}^{(i+1)}(z_i) = \mathrm{P}_{up}^{(i+1)} \mathbf{A}_{up}^{(i+1)}(z_{i+1}), \tag{3.23a}$$

$$\mathbf{A}_{down}^{(i+1)}(z_{i+1}) = \mathrm{P}_{down}^{(i+1)} \mathbf{A}_{down}^{(i+1)}(z_i), \tag{3.23b}$$

where propagation matrices are diagonal with eigenvalues as a argument in exponential factor:

$$\mathrm{P}_{up}^{(i+1)} = \exp\left(-\mathrm{i} k_0 d_{i+1} \mathrm{V}_{up}\right), \tag{3.24a}$$

$$\mathrm{P}_{down}^{(i+1)} = \exp\left(\mathrm{i} k_0 d_{i+1} \mathrm{V}_{down}\right), \tag{3.24b}$$

the parameter d_{i+1} is the thickness of layer. Relations (3.24) used in (3.21) leads to relation between waves on upper medium and waves propagated though interface and layer material:

$$\begin{bmatrix} \mathbf{A}_{up}^{(i)}(z_i) \\ \mathbf{A}_{down}^{(i+1)}(z_{i+1}) \end{bmatrix} = \tilde{\mathrm{s}}^{(i)} \begin{bmatrix} \mathbf{A}_{up}^{(i+1)}(z_{i+1}) \\ \mathbf{A}_{down}^{(i)}(z_i) \end{bmatrix}, \tag{3.25}$$

and $\tilde{s}^{(i)}$ is a matrix describing the continuity on interface and the propagation through layer:

$$\tilde{\mathrm{s}}^{(i)} = \begin{bmatrix} \tilde{\mathrm{s}}_{11}^{(i)} & \tilde{\mathrm{s}}_{12}^{(i)} \\ \tilde{\mathrm{s}}_{21}^{(i)} & \tilde{\mathrm{s}}_{22}^{(i)} \end{bmatrix} = \begin{bmatrix} \mathrm{s}_{11}^{(i)} \mathrm{P}_{up}^{(i+1)} & \mathrm{s}_{12}^{(i)} \\ \mathrm{P}_{down}^{(i+1)} \mathrm{s}_{21}^{(i)} \mathrm{P}_{up}^{(i+1)} & \mathrm{P}_{down}^{(i+1)} \mathrm{s}_{22}^{(i)} \end{bmatrix} \tag{3.26}$$

If the structure has only one planar interface, the problem is solved with matrix (3.26) for $d_{i+1} = 0$. The Matrix $\tilde{\mathrm{s}}^{(i+1)}$ can be also calculated for following interfaces (for example (z_{i+1}), see Figure 12.). Problem is with input and output amplitudes vectors which are bundled with inner interface, but goal of calculation is to get relation between input and output amplitudes (Figure 11). This problem can be solved with recurrent relation step by step connecting $\tilde{\mathrm{s}}^{(k)}, \quad k = 1, 2, \cdots, n < N$ matrices together with resulting $\mathrm{S}^{(n)}$-matrix:

$$\begin{bmatrix} \mathbf{A}_{up}^{(0)}(z_0) \\ \mathbf{A}_{down}^{(n+1)}(z_{n+1}) \end{bmatrix} = \mathrm{S}^{(n)} \begin{bmatrix} \mathbf{A}_{up}^{(n+1)}(z_{n+1}) \\ \mathbf{A}_{down}^{(0)}(z_0) \end{bmatrix}, \tag{3.27}$$

where matrix $\mathrm{S}^{(n)}$:

$$\mathrm{S}^{(n)} = \begin{bmatrix} \mathrm{S}_{11}^{(n)} & \mathrm{S}_{12}^{(n)} \\ \mathrm{S}_{21}^{(n)} & \mathrm{S}_{22}^{(n)} \end{bmatrix}. \tag{3.28}$$

Components of $\mathrm{S}^{(n+1)}$ are recurrently defined:

$$\begin{aligned}
\mathrm{S}_{11}^{(n+1)} &= \mathrm{S}_{11}^{(n)} \left[\mathbb{I} - \tilde{\mathrm{s}}_{12}^{(n+1)} \mathrm{S}_{21}^{(n)}\right]^{-1} \tilde{\mathrm{s}}_{11}^{(n+1)}, \\
\mathrm{S}_{12}^{(n+1)} &= \mathrm{S}_{12}^{(n)} + \mathrm{S}_{11}^{(n)} \left[\mathbb{I} - \tilde{\mathrm{s}}_{12}^{(n+1)} \mathrm{S}_{21}^{(n)}\right]^{-1} \tilde{\mathrm{s}}_{12}^{(n+1)} \mathrm{S}_{22}^{(n)}, \\
\mathrm{S}_{21}^{(n+1)} &= \tilde{\mathrm{s}}_{12}^{(n)} + \tilde{\mathrm{s}}_{22}^{(n+1)} \mathrm{S}_{21}^{(n)} \left[\mathbb{I} - \tilde{\mathrm{s}}_{12}^{(n+1)} \mathrm{S}_{21}^{(n)}\right]^{-1} \tilde{\mathrm{s}}_{11}^{(n+1)}, \\
\mathrm{S}_{22}^{(n+1)} &= \tilde{\mathrm{S}}_{22}^{(n)} \left[\mathrm{S}_{21}^{(n)} \left[\mathbb{I} - \tilde{\mathrm{s}}_{12}^{(n+1)} \mathrm{S}_{21}^{(n)}\right]^{-1} \tilde{\mathrm{s}}^{(n+1)}\right] \mathrm{S}_{22}^{(n)}.
\end{aligned} \tag{3.29}$$

Applying recursive formula to all layers in structure is obtained global scattering matrix S:

$$\begin{bmatrix} (A)_{up}^{(0)}(z_0) \\ (A)_{down}^{(N)}(z_N) \end{bmatrix} = \mathrm{S} \begin{bmatrix} (A)_{up}^{(N)}(z_N) \\ (A)_{down}^{(0)}(z_0) \end{bmatrix} \tag{3.30}$$

3.1.3 Reflection coefficients

Elements in S-matrix (3.30) directly represents the transmission and the reflection coefficients which can be easy determined from the expanded form of equation:

$$\begin{bmatrix} (A)_{S_{up}}^{(0)}(z_0) \\ (A)_{P_{up}}^{(0)}(z_0) \\ (A)_{S_{down}}^{(N)}(z_N) \\ (A)_{P_{down}}^{(N)}(z_N) \end{bmatrix} = \begin{bmatrix} S_{11} & S_{12} & S_{13} & S_{14} \\ S_{21} & S_{22} & S_{23} & S_{24} \\ S_{31} & S_{32} & S_{33} & S_{34} \\ S_{41} & S_{42} & S_{43} & S_{44} \end{bmatrix} \begin{bmatrix} (A)_{S_{up}}^{(N)}(z_N) \\ (A)_{P_{up}}^{(N)}(z_N) \\ (A)_{S_{down}}^{(0)}(z_0) \\ (A)_{P_{down}}^{(0)}(z_0) \end{bmatrix}. \tag{3.31}$$

Following the computing defined in Section 2.5.1 (where the reflection coefficients were calculated from M-matrix) are obtained forward reflection and transmission coefficients:

$$\begin{aligned}
r_{ss} &= S_{13} \qquad t_{ss} = S_{33}, \\
r_{ps} &= S_{14} \qquad t_{ps} = S_{34}, \\
r_{sp} &= S_{23} \qquad t_{sp} = S_{43}, \\
r_{pp} &= S_{24} \qquad t_{pp} = S_{44},
\end{aligned}$$

the backward reflection and transmission coefficients:

$$\begin{aligned}
r_{ss} &= S_{31} \qquad t_{ss} = S_{11}, \\
r_{ps} &= S_{32} \qquad t_{ps} = S_{12}, \\
r_{sp} &= S_{41} \qquad t_{sp} = S_{21}, \\
r_{pp} &= S_{42} \qquad t_{pp} = S_{22},
\end{aligned}$$

It is necessary take into consideration that reflection coefficients (3.35) are now matrices with the size $(2N+1 \times 2N+1)$ and their elements are reflection coefficients for all diffraction

orders. In most cases the specular reflection coefficients corresponding to zero diffraction order are needed. Absolute position of them in S is:

$$r_{ss} = [\mathrm{S}]_{N+1,5N+3}\,, \tag{3.32}$$
$$r_{ps} = [\mathrm{S}]_{N+1,7N+4}\,, \tag{3.33}$$
$$r_{sp} = [\mathrm{S}]_{3N+2,5N+3}\,, \tag{3.34}$$
$$r_{pp} = [\mathrm{S}]_{3N+2,7N+4}\,. \tag{3.35}$$

3.1.4 Fourier factorization

The S-matrix algorithm presented in previous section completely eliminate problems with numerical stability and theoretically for infinite Fourier series, but there is a problem with convergence for *p*-polarized waves, especially for highly absorbing grating material like metals, if the Fourier series are truncated. Problem comes from situation when the product of two multiplied discontinuous function at the same point is continuous function, $h\left(y\right) = f\left(y\right)g\left(y\right)$. If all function has the same period Λ than Fourier image of equation is:

$$\sum_{\infty}^{j=-\infty} h_j \exp\left(\mathrm{i}j\frac{2\pi}{\Lambda}y\right) = \sum_{\infty}^{k=-\infty} f_k \exp\left(\mathrm{i}k\frac{2\pi}{\Lambda}y\right) \cdot \sum_{\infty}^{l=-\infty} g_l \exp\left(\mathrm{i}l\frac{2\pi}{\Lambda}y\right). \tag{3.36}$$

Right side of equation can be simplified according to Laurent rule: product of two multiplied function is discrete convolution of their Fourier images:

$$\forall j \in \mathbb{Z}: \quad h_j = \sum_{\infty}^{k=-\infty} f_k g_{j-k} = \sum_{\infty}^{k=-\infty} f_{j-k} g_j. \tag{3.37}$$

Electric field and electric flux vectors are in relation:

$$\begin{bmatrix} \mathbf{D}_x \\ \mathbf{D}_y \\ \mathbf{D}_z \end{bmatrix} = \begin{bmatrix} \varepsilon_{xx} & \varepsilon_{xy} & \varepsilon_{xz} \\ \varepsilon_{yx} & \varepsilon_{yy} & \varepsilon_{yz} \\ \varepsilon_{zx} & \varepsilon_{zy} & \varepsilon_{zz} \end{bmatrix} \begin{bmatrix} \mathbf{E}_x \\ \mathbf{E}_y \\ \mathbf{E}_z \end{bmatrix}. \tag{3.38}$$

Now the problem is, that permititity tensor is discontinuous and field and flux components $\mathbf{E}_y$, $\mathbf{D}_x$ and $\mathbf{D}_z$ are discontinuous too. Components $\mathbf{E}_x$, $\mathbf{E}_z$ and $\mathbf{D}_y$ are continuous. For correct application of Laurent rule is need to reorganize equation (3.38) into form *discontinuous = discontinuous × continuous*:

$$\begin{bmatrix} \mathbf{D}_x \\ \mathbf{D}_z \\ \mathbf{E}_y \end{bmatrix} = \mathrm{B} \begin{bmatrix} \mathbf{E}_x \\ \mathbf{E}_z \\ \mathbf{D}_y \end{bmatrix}, \tag{3.39}$$

where:

$$\mathrm{B} = \begin{bmatrix} \varepsilon_{xx} - \varepsilon_{xy}\varepsilon_{yy}^{-1}\varepsilon_{yx} & \varepsilon_{xz} - \varepsilon_{xy}\varepsilon_{yy}^{-1}\varepsilon_{yz} & \varepsilon_{xy}\varepsilon_{yy}^{-1} \\ \varepsilon_{zx} - \varepsilon_{zy}\varepsilon_{yy}^{-1}\varepsilon_{yx} & \varepsilon_{zz} - \varepsilon_{zy}\varepsilon_{yy}^{-1}\varepsilon_{yz} & \varepsilon_{zy}\varepsilon_{yy}^{-1} \\ -\varepsilon_{yy}^{-1}\varepsilon_{yx} & -\varepsilon_{yy}^{-1}\varepsilon_{yz} & \varepsilon_{yy}^{-1} \end{bmatrix}. \tag{3.40}$$

This material tensor can be expanded according to number of calculation diffraction orders and transformed into Toeplitz form. Because our problem has to accord relation between electric flux and field (3.38), system of equation (3.40) is reassembled into previous form:

$$\begin{bmatrix} \lceil \mathbf{D}_x \rceil \\ \lceil \mathbf{D}_y \rceil \\ \lceil \mathbf{D}_z \rceil \end{bmatrix} = \mathrm{Q} \begin{bmatrix} \lceil \mathbf{E}_x \rceil \\ \lceil \mathbf{E}_y \rceil \\ \lceil \mathbf{E}_z \rceil \end{bmatrix}, \tag{3.41}$$

where:

$$\mathrm{Q} = \begin{bmatrix} \left[\!\left[\varepsilon_{xx} - \varepsilon_{xy}\varepsilon_{yy}^{-1}\varepsilon_{yx}\right]\!\right] - \left[\!\left[\varepsilon_{xy}\varepsilon_{yy}^{-1}\right]\!\right]\left[\!\left[\varepsilon_{yy}^{-1}\right]\!\right]^{-1}\left[\!\left[\varepsilon_{yy}^{-1}\varepsilon_{yx}\right]\!\right] & \left[\!\left[\varepsilon_{xy}\varepsilon_{yy}^{-1}\right]\!\right]\left[\!\left[\varepsilon_{yy}^{-1}\right]\!\right]^{-1} & \vdots \\ -\left[\!\left[\varepsilon_{yy}^{-1}\right]\!\right]^{-1}\left[\!\left[\varepsilon_{yy}^{-1}\varepsilon_{yx}\right]\!\right] & \left[\!\left[\varepsilon_{yy}^{-1}\right]\!\right]^{-1} & \vdots \\ \left[\!\left[\varepsilon_{zx} - \varepsilon_{zy}\varepsilon_{yy}^{-1}\varepsilon_{yx}\right]\!\right] - \left[\!\left[\varepsilon_{zy}\varepsilon_{yy}^{-1}\right]\!\right]\left[\!\left[\varepsilon_{yy}^{-1}\right]\!\right]^{-1}\left[\!\left[\varepsilon_{yy}^{-1}\varepsilon_{yx}\right]\!\right] & \left[\!\left[\varepsilon_{zy}\varepsilon_{yy}^{-1}\right]\!\right]\left[\!\left[\varepsilon_{yy}^{-1}\right]\!\right]^{-1} & \vdots \end{bmatrix}$$

$$\begin{bmatrix} \vdots & \left[\!\left[\varepsilon_{xz} - \varepsilon_{xy}\varepsilon_{yy}^{-1}\varepsilon_{yz}\right]\!\right] - \left[\!\left[\varepsilon_{xy}\varepsilon_{yy}^{-1}\right]\!\right]\left[\!\left[\varepsilon_{yy}^{-1}\right]\!\right]^{-1}\left[\!\left[\varepsilon_{yy}^{-1}\varepsilon_{yz}\right]\!\right] \\ \vdots & -\left[\!\left[\varepsilon_{yy}^{-1}\right]\!\right]^{-1}\left[\!\left[\varepsilon_{yy}^{-1}\varepsilon_{yz}\right]\!\right] \\ \vdots & \left[\!\left[\varepsilon_{zz} - \varepsilon_{zy}\varepsilon_{yy}^{-1}\varepsilon_{yz}\right]\!\right] - \left[\!\left[\varepsilon_{zy}\varepsilon_{yy}^{-1}\right]\!\right]\left[\!\left[\varepsilon_{yy}^{-1}\right]\!\right]^{-1}\left[\!\left[\varepsilon_{yy}^{-1}\varepsilon_{yz}\right]\!\right] \end{bmatrix} \tag{3.42}$$

Matrix Q is now used instead of Toeplitz permitivity tensor matrix wit better convergence as a result (see Example 3.2.1.).

3.2 Numerical experiments

3.2.1 Convergence test for Fourier factorization

The truncation of Fourier series brings an inaccuracy into the calculated data. It can be improved by calculating with more diffraction orders, but it increase calculating time and more memory is needed to get better convergence. Fourier factorization method is a trick how to improve convergence to spend computing time or get more accurate results. The number of the diffraction orders which gives accurate result and has not too big requirement to the memory and time is appropriate to known. Following graphs has been calculated for the angle of incidence $\phi = 45°$, the wavelength $\lambda = 400\,nm$, f denotes filling factor:

$$\hat{\epsilon}\,(y) = \begin{cases} 1 & \text{for} \quad y \in \langle 0, f\Lambda) \\ 7 & y \in \langle f\Lambda, (1-f)\,\Lambda\rangle \end{cases}, \tag{3.43}$$

the period of grating $\Lambda = 1000\,nm$, thickness $10\,nm$ and a air ($\epsilon = 1$) as a substrate and a superstrate the same.
On Figure 13 we can see, that for the calculating without factorization is needed almost 80 diffraction orders to obtain precise calculation for the *p*-polarized light. On the other hand, if the factorization is applied 30 diffraction orders is enough and further increase does not increase calculated precision. This convergence analysis should be done for each calculating structure.

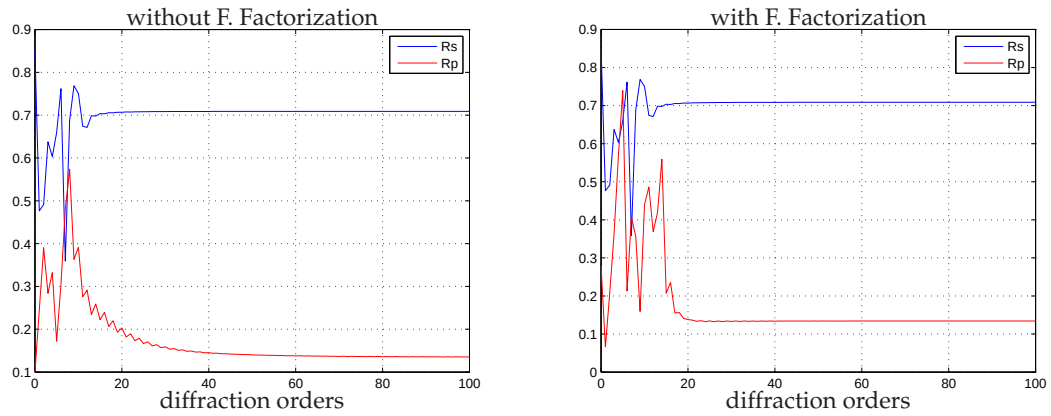

Figure 13: Comparison convergence speed without and with applied Fourier factorization method in model.

3.2.2 Dependecy of reflectance on a simple grating layer with the variable fill-factor

Following graphs has been calculated for the angle of incidence $\phi = 45°$, the wavelength $\lambda = 400nm$ and the variable fill factor $f \in \langle 0, 1\rangle$, period of grating $\Lambda = 100nm$:

$$\hat{\epsilon}\left(y\right) = \begin{cases} 1 \quad \text{for} \quad y \in \langle 0, f\Lambda) \\ 7 \qquad y \in \langle f\Lambda, (1-f)\,\Lambda\rangle \end{cases}, \tag{3.44}$$

thickness $100nm$ and a the air ($\epsilon = 1$) as a superstrate and the substrate with $\epsilon = 7$.

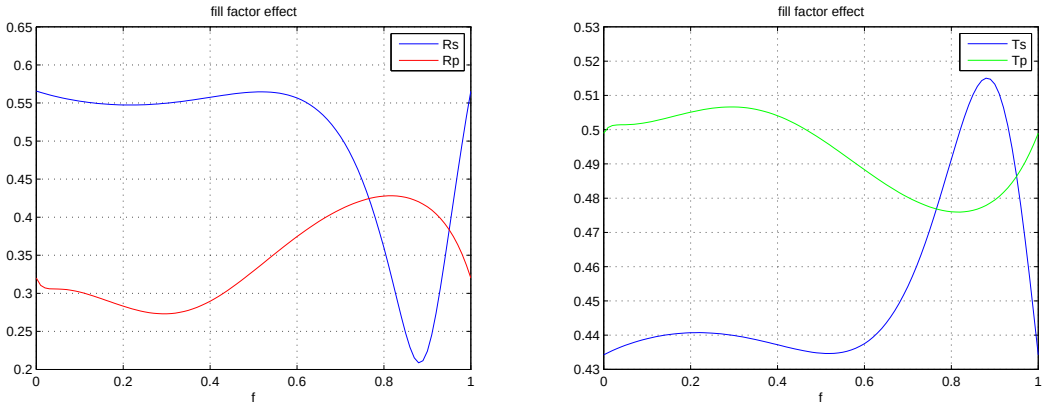

Figure 14: Dependency of specular from grating on the fill factor

Figure 14. shows dependency of the reflectance and transmittance as a function of the fill factor f. The model were observed for $N = 30$ and the Fourier factorization was used. The first and last points of graph has the same value, because for fill factor $f = \{0, 1\}$ the grating degrades into homogeneous layer with the interface between medium with the $\epsilon = 1$ and $\epsilon = 7$.

3.2.3 Nonreciprocal periodic structure

Limitation of actual optical insulator conception is interface between the integrated part of device and the optical insulator and from that comes the idea of the integrated optical insulator into one chip together with laser diode, modulating device, multiplexer, etc. Problem of he integrated conception is in usable materials, because the optical properties of natural materials are in the contradiction with required properties for the integration.

There are two essential properties, the first is magneto-optic (MO) effect and the second is losslessness. Magnetic garnet is a material with low losses bud with small MO effect. Metals have big MO effect but also big losses. From that contradiction comes out the idea of designing new material with the big magneto-optic effect and small losses and can be used in integrated optical insulator [13, 14].
Figure 15. shows elements (one period) of the hexagonal modeled structure for wavelength $\lambda = 1300nm$

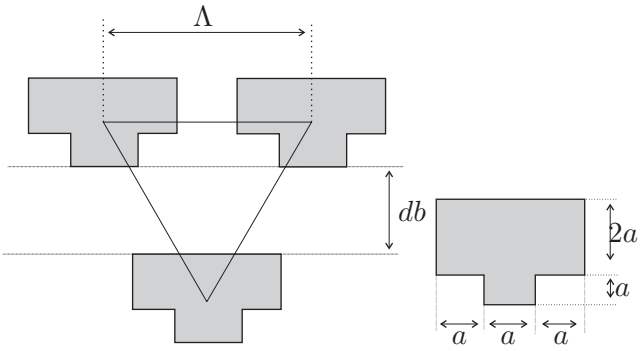

Figure 15: Scheme of photonics crystal structure.

where:

$$\begin{aligned} f &= 0.4548 \\ \Lambda &= f\lambda = 591.24nm \\ a &= \tfrac{f\Lambda}{3} = 89.632nm \\ db &= 33.276nm \end{aligned}$$

Structure has been calculated for the 12 period shown on the Figure 15. The *T*-shaped elements are air holes with the permitivity $\epsilon = 1$ was surrounded and separated (gap with thickness *db*) with the magnetic garnet:

$$\epsilon_{m\_garnet} = \begin{bmatrix} n^2 & 0 & 0 \\ 0 & n^2 & i\,\varepsilon_1 \\ 0 & -i\,\varepsilon_1 & n^2 \end{bmatrix}, \tag{3.45}$$

where $n = 2.25$ and $\epsilon_1 = 0.1$. Superstrate and substrate was nonmagnetic garnet with refractive index $n = 2.25$.
On the Figure 17. is enlarged area with big difference between forward and backward transmission coefficients for *p*-polarized wave.

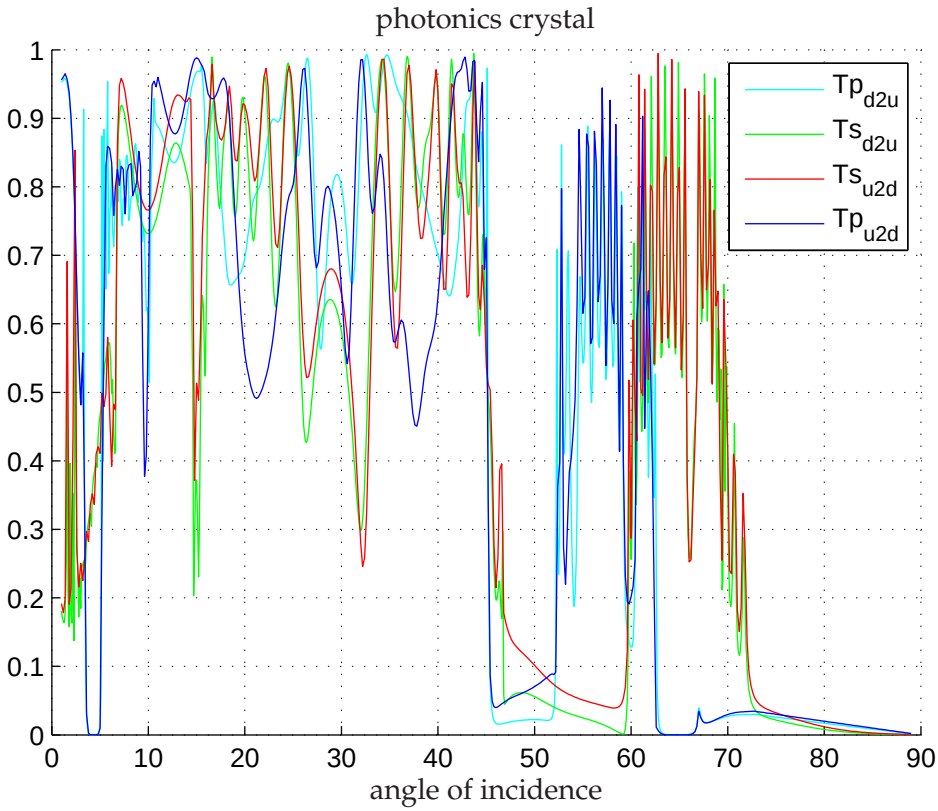

Figure 16: Transmission coefficient for forward and backward propagation in photonics crystal.

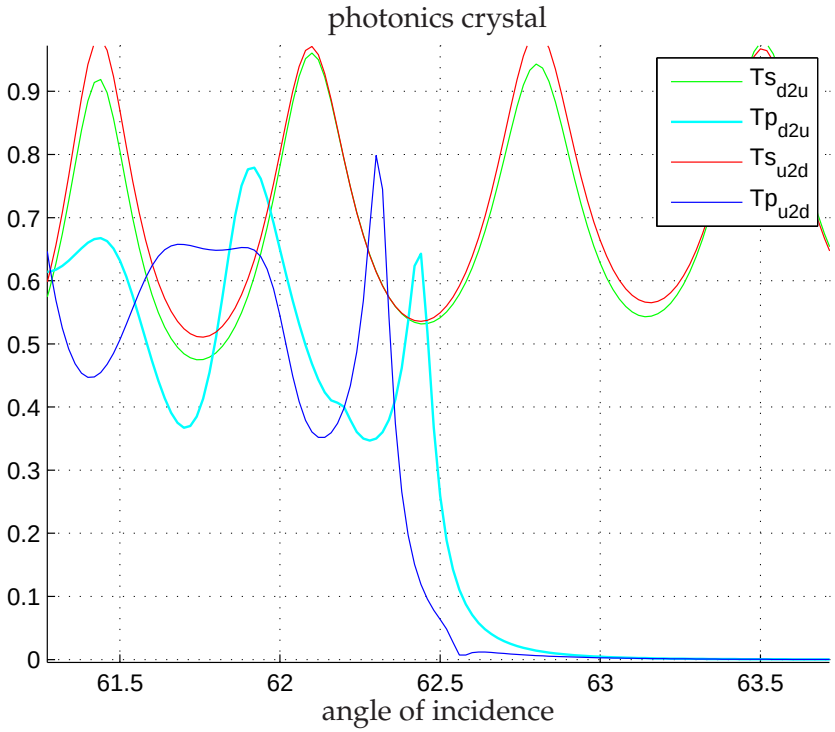

Figure 17: Detail of difference between forward and backward propagation constant for angle of incidence $\phi = 62.44°$.

4 Ellipsometric response from anisotropic medium

Spectroscopic ellipsometry is an optical method for characterization of the sample optical properties. This method is based on the detection of changes in reflected polarized light from sample, Figure 18. If the sample is isotropic sample the polarization state change is expressed with the ellipsometric angles ψ and Δ. If the sample is anisotropic the problem becomes more complex because one pair of ellipsometric angles ψ and Δ is not enough and more advanced method, generalized ellipsometry is needed([9, 15, 16]).

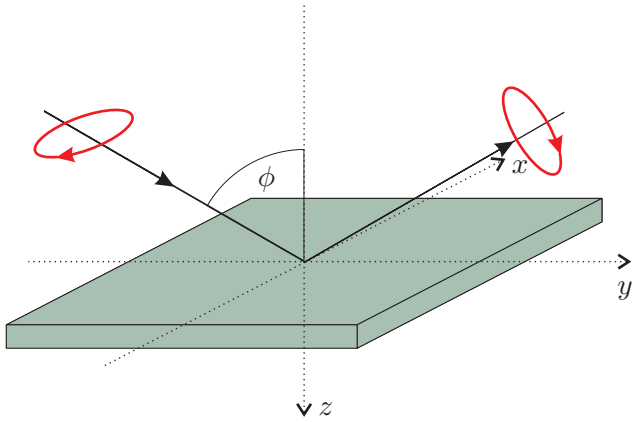

Figure 18: Light polarization state change after reflection from sample.

4.1 Matrix description of ellipsometer optical system with anisotropic sample

In further text will be described face-modulation ellipsometer Uvisel, Horiba Jobin Yvon in configuration polarizer-sample-modulator-analyzer (PCMA) with Jones matrix formalism providing nondepolarizing sample.

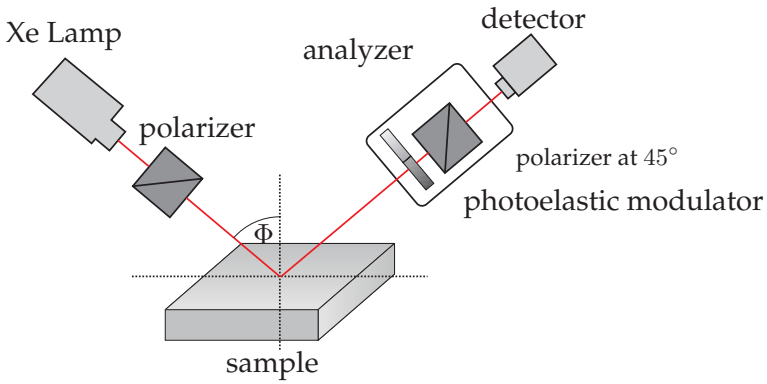

Figure 19: Ellipsometer configuration is shown schematically.

Anisotropic nondepolarizing sample is described using the Jones matrix:

$$\begin{bmatrix} r_{ss} & r_{ps} \\ r_{sp} & r_{pp} \end{bmatrix} \propto \begin{bmatrix} 1 & \frac{r_{ps}}{r_{ss}} \\ \frac{r_{sp}}{r_{ss}} & \frac{r_{pp}}{r_{ss}} \end{bmatrix}, \tag{4.1}$$

whose normalized form (right side) defines free complex ratios and three pairs of the ellipsometric angles connect with them. First is the same as in ellipsometry o isotropic materials:

$$\chi_0 = \frac{r_{pp}}{r_{ss}} = \tan\psi_0\, \mathrm{e}^{i\Delta_0}, \tag{4.2}$$

and another two $r_{ps}/r_{ss} = \tan\psi_{ps}\mathrm{e}^{\mathrm{i}\Delta_{ps}}$ and $r_{sp}/r_{ss}\tan\psi_{sp}\mathrm{e}^{\mathrm{i}\Delta_{sp}}$, which will ensue from following matrix description. Firstly the complete matrix description of ellipsometer using Jones matrix formalism is in a form:

$$\mathbf{A} = \frac{1}{\sqrt{2}}\begin{bmatrix} 1 & 0 \\ 0 & 0 \end{bmatrix}\begin{bmatrix} \mathrm{e}^{i\frac{\varphi}{2}} & -\mathrm{e}^{-i\frac{\varphi}{2}} \\ \mathrm{e}^{i\frac{\varphi}{2}} & \mathrm{e}^{-i\frac{\varphi}{2}} \end{bmatrix}\begin{bmatrix} \sin M & \cos M \\ -\cos M & \sin M \end{bmatrix}\begin{bmatrix} r_{ss} & r_{ps} \\ r_{sp} & r_{pp} \end{bmatrix}\begin{bmatrix} \sin P \\ \cos P \end{bmatrix}, \tag{4.3}$$

where M is azimuthal angle of photoelastic modulator fixtly linked to analyzer at 45° and both components rotate together as one component called modulator, P is the azimuthal angle of polarizer, (Figure 19.). Amplitude $\mathbf{A}$ on detector is easy to determine with the substitutions:

$$a = (r_{ss}\sin P + r_{ps}\cos P)\sin M + (r_{sp}\sin P + r_{pp}\cos P)\cos M, \tag{4.4a}$$
$$b = (r_{sp}\sin P + r_{pp}\cos P)\sin M - (r_{ss}\sin P + r_{ps}\cos P)\cos M, \tag{4.4b}$$

and the final amplitude product:

$$\mathbf{A} = \frac{1}{\sqrt{2}}\left(a\mathrm{e}^{i\frac{\varphi}{2}} - b\mathrm{e}^{-i\frac{\varphi}{2}}\right). \tag{4.5}$$

Because nor amplitude $\mathbf{A}$ the equation (4.5) is measurable only the intensity I we have to multiply with its complex conjugate form and result can be written:

$$I = \underbrace{\frac{1}{2}(aa^* + bb^*)}_{I_0} + \underbrace{i\frac{1}{2}(ba^* - ab^*)}_{I_1}\sin\varphi - \underbrace{\frac{1}{2}(ab^* + ba^*)}_{I_2}\cos\varphi. \tag{4.6}$$

Value I_0 is the DC component of signal, I_1 and I_2 are are the signals detected on modulation the frequency $f = 50\mathrm{kHz}$ and on second harmonics frequency 2ω. For elimination of fluctuating intensity is measured ratios of modulated and DC signal components:

$$I_S = \frac{I_1}{I_0} \quad \text{a} \quad I_C = \frac{I_2}{I_0}. \tag{4.7}$$

4.1.1 Measured signal I_S and I_C from anisotropic sample

For the different configuration of azimuthal angles P and M the measured signals represents different elements (or their combination) of samples reflection matrix. Commonly are used following combinations of angles:

$$P \in \{0^\circ, 90^\circ, 45^\circ, -45^\circ\} \quad M \in \{0^\circ, 90^\circ, 45^\circ, -45^\circ\}. \tag{4.8}$$

Evaluating (4.7) with the angles P and M (4.8) the I_S and I_C signals express products of reflection coefficients, notation $I_S^{P,M}$ or $I_C^{P,M}$ is used:

$$I_S^{45,M} = -i\frac{(r_{ss}+r_{ps})(r_{pp}+r_{sp})^* - \mathbf{c.c.}}{|r_{ss}+r_{ps}|^2 + |r_{pp}+r_{sp}|^2}, \tag{4.9a}$$

$$I_S^{-45,M} = i\frac{(r_{ss}-r_{ps})(r_{pp}-r_{sp})^* - \mathbf{c.c.}}{|r_{ss}-r_{ps}|^2 + |r_{pp}-r_{sp}|^2}, \tag{4.9b}$$

$$I_S^{0,M} = i\frac{\left(r_{pp}r_{ps}^*\right) - \left(r_{ps}r_{pp}^*\right)}{|r_{ps}|^2 + |r_{pp}|^2}, \tag{4.9c}$$

$$I_S^{90,M} = i\frac{\left(r_{sp}r_{ss}^*\right) - \left(r_{ss}r_{sp}^*\right)}{|r_{ss}|^2 + |r_{sp}|^2}, \tag{4.9d}$$

$$I_C^{45,0} = -I_C^{45,90} = \frac{(r_{ss}+r_{ps})(r_{pp}+r_{sp})^* + \mathbf{c.c.}}{|r_{ss}+r_{ps}|^2 + |r_{pp}+r_{sp}|^2}, \tag{4.10a}$$

$$I_C^{-45,0} = -I_C^{-45,90} = \frac{(r_{ss}-r_{ps})(r_{pp}-r_{sp})^* + \mathbf{c.c.}}{|r_{ss}-r_{ps}|^2 + |r_{pp}-r_{sp}|^2}, \tag{4.10b}$$

$$I_C^{45,45} = -I_C^{45,-45} = \frac{|r_{ss}+r_{ps}|^2 + |r_{ss}+r_{ps}|^2}{|r_{ss}+r_{ps}|^2 + |r_{pp}+r_{sp}|^2}, \tag{4.10c}$$

$$I_C^{-45,45} = -I_C^{-45,-45} = \frac{|r_{ss}-r_{ps}|^2 + |r_{ss}-r_{ps}|^2}{|r_{ss}-r_{ps}|^2 + |r_{pp}-r_{sp}|^2}, \tag{4.10d}$$

$$I_C^{0,0} = -I_C^{0,90} = \frac{r_{pp}r_{ps}^* + r_{ps}r_{pp}^*}{|r_{pp}|^2 + |r_{ps}|^2}, \tag{4.10e}$$

$$I_C^{90,0} = -I_C^{90,90} = \frac{r_{sp}r_{ss}^* + r_{ss}r_{sp}^*}{|r_{ss}|^2 + |r_{sp}|^2}, \tag{4.10f}$$

$$I_C^{0,45} = -I_C^{0,-45} = -\frac{|r_{pp}|^2 - |r_{ps}|^2}{|r_{pp}|^2 + |r_{ps}|^2}, \tag{4.10g}$$

$$I_C^{90,45} = -I_C^{90,-45} = -\frac{|r_{ss}|^2 - |r_{sp}|^2}{|r_{ss}|^2 + |r_{sp}|^2}, \tag{4.10h}$$

where **c. c.** is the complex conjugate number.

4.2 Experimental data

The experimental data were measured on the SnO_2 crystal with expected tetragonal crystal structure for photon energy 3.9eV (3179nm) and angle of incidence $60°$. This type of structure corresponds with uniaxial optical anisotropy (2.17). Inducement for recognition of off-diagonal elements in reflection matrix is the signal I_S and I_C for the configuration $P = 0°, P = 0°$, (4.9c,4.10e), incident wave is p-polarized. Thus signals are for isotropic medium equal to the zero, but for uniaxal anisotropy they are nonzero and depends on azimuthal angle of sample rotation.

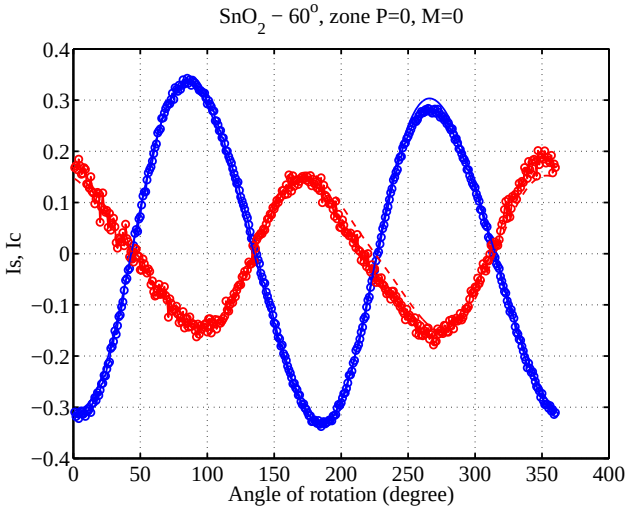

Figure 20: Effect of the uniaxial optical anisotropy in ellipsometric data as a function of azimuthal rotation.

In the measured data are four significant points where the lines cross each other, Figure 20. For these angles of azimuthal rotation of the sample are axes of the rotation symmetry parallel or perpendicular to the plane of incidence light and effect of anisotropy disappears. In this configuration we can measure sample with the classical ellipsometric method.

5 Conclusion and perspectives

Main contribution of this master thesis are:

- understood of Berreman and Yeh approach for solving Maxwell equation in layered media,
- implemented program in MATLAB software for modeling optical response from the structure of planar layers and the lammelar (1D) gratings,
- modeled of planar layered medium with the plasmon resonance,
- designed and modeled photonics crystal structure with the non-reciprocity effect: hight transmission in forward direction and strong attenuation in backward direction,
- measurement technique for characterization uniaxial optical crystal anisotropy.

Goals for future work:

- understanding to calculation process for more general grating profile: saw-like, sinusoidal, etc.,
- calculation of two-dimensional (2D) gratings,
- optimisation of phototonics crystal structure for better isolating ratio.

6 List of publications

L. Halagačka, K. Postava, M. Foldyna, and J. Pištora. *Precise phase-modulation generalized ellipsometry of anizotropic samples*. Physica Status Solidi (a)**205**, 752-755 (2008).

K. Postava. **L. Halagačka**, D. Hrabovský, O. Životský, J. Pištora, D. Pawlak, D. A. Turczynski, and S. Kolodzejak, *Optical spectroscopy of terbium-scandium-aluminium garnet and terbium-scandium perovskite*, Proc. of SPIE **7353**, 735311 (2009).

K. Postava, Y. Z Gao, X. Y. Gong, **L. Halagačka**, J. Pištora, A. Nakaoka, and T. Yamaguchi, *Spectroscopic ellipsometry of anodized layer on single crystal InAsSb layer grown by melt epitaxy*, Phys. Stat. Sol.(c) **5**, 1316-1319 (2008).

O. Životský, F. Fendrych, L. Kraus, K. Postava, **L. Halagačka**, and J. Pištora, *Soft magnetic properties of as-deposited FeCoAlN films studied using magneto-optic magnetometry*, J. Magn. Magn. Mater, **316**, e858-e861 (2007).

L. Halagačka, K. Postava, M. Foldyna, and J. Pištora: *Phase modulation generalized ellipsometry of anisotropic samples*. In: Annual Proceedings of Science and Technology at VŠB-TUO, part II, pp. 48-49, (2008).

7 References

[1] D. W. Berreman, *Optic in Stratifield and Anisotropic media:* 4×4*-Matrix Formulation* J. Opt. Soc. Am., **62**, 502-510, (1972).

[2] P. Yeh, *Electromagnetic propagation in birefringent layered media* J. Opt. Soc. Am., **69**, 742-756, (1979).

[3] L. Li, *Use of Fourier series in the analysis of discontinuous periodic structures* J. Opt. Soc. Am., **13**, 1870-1876, (1996).

[4] M. Foldyna, *Modeling of electromagnetic waves in anisotropic periodic structures*, PhD. Thesis, Technical University of Ostrava, 2005.

[5] L. Li, *Formulation and comparison of two recursive matrix algorithms for modeling layer diffraction gratings* J. Opt. Soc. Am., **13**, 1024-1035, (1996).

[6] L. Li, *Note on the* S*-matrix propagation algorithm* J. Opt. Soc. Am., **20**, 655-660, April 2003.

[7] R. M. A. Azzam and N. M. Bashara, *Ellipsometry and Polarized Light,* 2nd ed. (North-Holand, Amsterdam, 1987).

[8] K. Vedam, *Spectroscopic ellipsometry: a historical overview,* Thin Solid Films **313-314,**, 1-9 (1998).

[9] G. E. Jellison, Jr. and F. A Modine, *Two-modulation generalized ellipsometry: theory,* Appl. Opt. **36,** 8190-8189 (1997).

[10] K. Postava, T. Yamaguchi, and R. Kantor, *Matrix description of coherent and incoherent light reflection and transmission by anizotropic multilayer structures,* Appl. Opt. **41**, 2521-2531 (2002).

[11] P. Yeh, *Optical waves in layered media,* (John Willey & Sons, 1988).

[12] M. Neviere and E. Popov, *Light propagation in periodic media: Differential theory and design,* (Marcel Dekker, Inc. 2003).

[13] M. Vanwolleghem, Ph. Gogol, P. Beauvillain, W. Van Parys, and R. Baets. *Design and optimization of a monolithically integratable InP-based optical waveguide isolator*, J. Opt. Soc. Am. B, **24**, 94-105, 2007.

[14] J. M. Lourtiouz, H. Benisty, V. Berger, J.M. Gerard, D. Maystre, and A. Tchelnokov, *Photonic crystals: Towards nanoscale photonic devices,* (Springer, 2005).

[15] M. Schubert, T. E. Tiwald, and J. A. Woollam, *Explicit solutions for the optical properties of arbitrary magneto-optic materials in generalized ellipsometry*, Appl. Opt. **38**, 177–187 (1999).

[16] L. Halagačka, K. Postava, M. Foldyna, and J. Pištora, *Precise phase-modulation generalized ellipsometry of anisotropic samples* Phys. Stat. Sol. (a) **205**, No.4,752-755 (2008).